JOURNAL OF GEOPHYSICAL RESEARCH, VOL. 112, D05302, doi:10.1029/2006JD007801, 2007

Why are there large differences between models in global budgets of tropospheric ozone?

Shiliang Wu,[1] Loretta J. Mickley,[1] Daniel J. Jacob,[1] Jennifer A. Logan,[1] Robert M. Yantosca,[1] and David Rind[2]

Received 17 July 2006; revised 27 September 2006; accepted 6 November 2006; published 3 March 2007.

[1] Global 3-D tropospheric chemistry models in the literature show large differences in global budget terms for tropospheric ozone. The ozone production rate in the troposphere, $P(O_x)$, varies from 2300 to 5300 Tg yr^{-1} across models describing the present-day atmosphere. The ensemble mean of $P(O_x)$ in models from the post-2000 literature is 35% higher than that compiled in the Intergovernmental Panel on Climate Change (IPCC) Third Assessment Report (TAR). Simulations conducted with the GEOS-Chem model using two different assimilated meteorological data sets for 2001 (GEOS-3 and GEOS-4), as well as 3 years of GISS GCM meteorology, show $P(O_x)$ values in the range 4250–4700 Tg yr^{-1}; the differences appear mostly because of clouds. Examination of the evolution of $P(O_x)$ over the GEOS-Chem model history shows major effects from changes in heterogeneous chemistry, the lightning NO_x source, and the yield of organic nitrates from isoprene oxidation. Multivariate statistical analysis of model budgets in the literature indicates that 74% of the variance in $P(O_x)$ across models can be explained by differences in NO_x emissions, inclusion of nonmethane volatile organic compounds (NMVOCs, mostly biogenic isoprene), and ozone influx from stratosphere-troposphere exchange (STE). Higher NO_x emissions, more widespread inclusion of NMVOC chemistry, and weaker STE in the more recent models increase ozone production; however, the effect of NMVOCs does not appear generally sensitive to the magnitude of emissions within the range typically used in models (500–900 Tg C yr^{-1}). We find in GEOS-Chem that $P(O_x)$ saturates when NMVOC emissions exceed 200 Tg C yr^{-1} because of formation of organic nitrates from isoprene oxidation, providing an important sink for NO_x.

Citation: Wu, S., L. J. Mickley, D. J. Jacob, J. A. Logan, R. M. Yantosca, and D. Rind (2007), Why are there large differences between models in global budgets of tropospheric ozone?, *J. Geophys. Res.*, *112*, D05302, doi:10.1029/2006JD007801.

1. Introduction

[2] Tropospheric ozone is of importance in atmospheric chemistry as a greenhouse gas, as a precursor for the OH oxidant which controls the atmospheric lifetime of many gases, and as a surface air pollutant toxic to humans and vegetation. It is produced by photochemical oxidation of carbon monoxide, methane, and nonmethane volatile organic compounds (NMVOCs) in the presence of nitrogen oxide radicals ($NO_x \equiv NO + NO_2$), and is also supplied by transport from the stratosphere. It is removed by chemical reactions and by deposition. The lifetime of tropospheric ozone varies from days to months, and the lifetimes of the precursors span an even wider range, so that quantitative accounting of the factors controlling tropospheric ozone requires a global 3-D model that couples chemistry and transport on synoptic scales.

[3] A large number of global models for tropospheric ozone have been developed over the past decade, and the pre-2000 models were reviewed by the Intergovernmental Panel on Climate Change (IPCC) Third Assessment Report (TAR) [*Prather et al.*, 2001, Table 4.12]. More recent (post-2000) model studies are compiled in Table 1, and summary statistics across models of global tropospheric ozone budgets for present-day conditions are compiled in Table 2. Global burdens vary by only 10–20% among the models, but global production rates vary by more than 50%, suggesting that different models could give very different responses to perturbations. Global production rates averaged across all state-of-science models increased by 35% from the generation reviewed by the IPCC TAR to the post-2000 generation, and are higher still in the recent *Stevenson et al.* [2006] intercomparison of 21 global models. *Stevenson et al.* [2006] proposed that the higher ozone production rates in their study are due to several reasons including "(1) higher NO_x emissions, (2) higher isoprene emissions, (3) more detailed NMHC schemes, and possibly (4) improved parameteriza-

[1]Division of Engineering and Applied Sciences and Department of Earth and Planetary Sciences, Harvard University, Cambridge, Massachusetts, USA.
[2]NASA Goddard Institute for Space Studies, New York, New York, USA.

0148-0227/07/2006JD007801$09.00

Table 1. Global Model Budgets of Tropospheric Ozone in the Recent Literature[a]

Reference	Sources, Tg yr^{-1}		Sinks, Tg yr^{-1}		Burden, Tg	Lifetime,[c] days
	Chemical Production[b]	Stratospheric Influx	Chemical Loss[b]	Deposition		
Lelieveld and Dentener [2000]	3310	570	3170	710	350	33
Bey et al. [2001][d]	4900	470	4300	1070	320	22
Sudo et al. [2002]	4895	593	4498	990	322	21
Horowitz et al. [2003]	5260	340	4750	860	360	23
von Kuhlmann et al. [2003]	4560	540	4290	820	290	21
Shindell et al. [2003]	NR[e]	417	NR	1470	349	NR
Hauglustaine et al. [2004]	4486	523	3918	1090	296	22
Park et al. [2004b]	NR	480	NR	1290	340	NR
Rotman et al. [2004]	NR	660	NR	830	NR	NR
Wong et al. [2004]	NR	600	NR	1100	376	NR
Stevenson et al. [2004]	4980	395	4420	950	273	19
Wild et al. [2004]	4090	520	3850	760	283	22
Stevenson et al. [2006][f]	5110 ± 610	550 ± 170	4670 ± 730	1000 ± 200	340 ± 40	22 ± 2

[a]From global model simulations published since the IPCC TAR compilation and describing the atmosphere of the last decade of the 20th century.

[b]Chemical production and loss rates are calculated for the odd oxygen family, usually defined as $O_x \equiv O_3 + O + NO_2 + 2NO_3 + 3N_2O_5 +$ peroxyacetylnitrates (PANs) + HNO_3 + HNO_4, to avoid accounting for rapid cycling of ozone with short-lived species that have little implication for its budget. Chemical production is mainly contributed by reactions of NO with peroxy radicals, while chemical loss is mainly contributed by the $O(^1D) + H_2O$ reaction and by the reactions of ozone with HO_2, OH, and alkenes. Several models in this table do not report production and loss separately ("NR" entry in the table), reporting instead net production. However, net production is not a useful quantity for budget purposes because (1) it is a small residual between large production and loss, (2) it represents a balance between STE and dry deposition, both of which are usually parameterized to some degree as flux boundary conditions.

[c]Calculated as the ratio of the burden to the sum of chemical and deposition losses.

[d]A more recent version of GEOS-Chem by *Martin et al.* [2003b] gives identical rates and burdens.

[e]Not reported.

[f]Means and standard deviations from an intercomparison study of 21 global models constrained to use the same anthropogenic and biomass burning emissions for ozone precursors.

Table 2. Global Budgets of Tropospheric Ozone: Statistics Across Models[a]

	Sources, Tg yr^{-1}		Sinks, Tg yr^{-1}		Burden, Tg	Lifetime, days
	Chemical Production	Stratospheric Influx	Chemical Loss	Deposition		
IPCC TAR [*Prather et al.*, 2001]						
11 models[b]	3420 ± 770	770 ± 400	3470 ± 520	770 ± 180	300 ± 30	24 ± 2
Wang et al. [1998b][c]	4100	400	3680	820	310	25
Post-2000 literature (Table 1)[d]						
13 models	4620 ± 600	510 ± 90	4200 ± 480	1000 ± 220	330 ± 30	23 ± 4
GEOS-Chem[e]	4900	470	4300	1070	320	22
Stevenson et al. [2006][f]						
21 models	5110 ± 610	550 ± 170	4670 ± 730	1000 ± 200	340 ± 40	22 ± 2
GEOS-Chem[g]	4490	510	3770	1230	290	22
Our work (GEOS-Chem)[h]						
GEOS-3	4250	540	3710	1080	300	23
GEOS-4	4700	520	4130	1090	300	21
GISS[i]	4470 ± 10	510 ± 2	3990 ± 10	990 ± 10	320 ± 3	23 ± 0.4

[a]From global model simulations describing the present-day (post-1985) atmosphere. For the tropospheric ozone budgets reported in the literature, the chemical production and loss rates are calculated for the odd oxygen family (O_x) including species that cycle rapidly with ozone, while the other terms might be for either O_x or O_3. In our work all the budget terms are for O_x, which is defined as $O_x \equiv O_3 + O + NO_2 + 2 \times NO_3 + 3 \times N_2O_5 +$ PANs + HNO_3 + HNO_4 (with the molecular weight of O_x assumed to be the same as O_3 since O_3 accounts for over 95% of O_x) following *Wang et al.* [1998b] and *Bey et al.* [2001], and the tropopause is defined as the altitude at which the temperature lapse rate drops below 2 K km^{-1}. Other models may use different definitions of the O_x family and of the tropopause, as discussed in the text. Chemical production of ozone as computed in all models is mainly from the reactions of peroxy radicals with NO.

[b]Means and standard deviations from an ensemble of 11 global model budgets in the 1996–2000 literature.

[c]Precursor to GEOS-Chem model using NASA/GISS general circulation model (GCM) meteorological fields.

[d]Means and standard deviations from an ensemble of 13 global model simulations reported in the literature since the IPCC TAR (Table 1). Means from the *Stevenson et al.* [2006] intercomparison study are included as one value in that ensemble.

[e]Results reported by *Bey et al.* [2001] for GEOS-Chem version 3.02 (http://www.as.harvard.edu/chemistry/trop).

[f]Means and standard deviations from an intercomparison study of 21 global models constrained to use the same anthropogenic and biomass burning emissions for ozone precursors.

[g]Results from GEOS-Chem version 7.01.02 contributed to the *Stevenson et al.* [2006] intercomparison. The GEOS-Chem STE fluxes reported by *Stevenson et al.* [2006] are inferred as the residual of the chemistry and deposition terms, and are erroneously low because the deposition rate is given there as that of ozone only instead of O_x. We give here the correct GEOS-Chem budget for O_x.

[h]The three GEOS-Chem simulations reported here differ only in the driving meteorological fields (GEOS-3 and GEOS-4 assimilated meteorological observations for 2001, GISS GCM output for 3 years of the present-day climate).

[i]Means and interannual standard deviations from 3 years of simulations.

Table 3. Global Emissions of Ozone Precursors in the GEOS-Chem Model[a]

Species	Emission Rate
NO_x, Tg N yr^{-1}	43.8
Fossil fuel combustion	23.6
Biomass burning	6.5
Biofuel	2.2
Soil	6.3
Lightning	4.7
Aircraft	0.5
CO, Tg CO yr^{-1}	1034
Fossil fuel combustion	403
Biomass burning	457
Biofuel	173
Ethane, Tg C yr^{-1}	8.7
Anthropogenic emissions	6.8
Biomass burning	1.9
Propane, Tg C yr^{-1}	10.9
Anthropogenic emissions	10.2
Biomass burning	0.7
$\geq C_4$ alkanes, Tg C yr^{-1}	25.8
Anthropogenic emissions	24.4
Biomass burning	0.6
Biofuel	0.8
$\geq C_3$ alkenes, Tg C yr^{-1}	27.8
Anthropogenic emissions	8.8
Biomass burning	7.5
Biogenic emissions	11.5
Isoprene from vegetation, Tg C yr^{-1}	400
Monoterpenes from vegetation, Tg C yr^{-1}	110
Acetone, Tg C yr^{-1}	44.4
Anthropogenic emissions	0.7
Biomass burning	3.1
Biogenic emissions	40.6

[a]Anthropogenic emissions are for 1995. Fixed methane concentrations of 1706, 1710, 1768, and 1823 ppbv are imposed for 90–30°S, 30°S–0°, 0°–30°N, and 30–90°N.

tions of processes such as photolysis, convection, and stratosphere-troposphere exchange''; their sensitivity study with one model (FRSGC/UCI) showed that the increase of NO_x and isoprene emissions can each explain roughly half of the increase of ozone production rate for that model compared to results compiled in IPCC TAR.

[4] We present here a more thorough investigation of differences among model ozone budgets through multivariate statistical analyses of tropospheric ozone budgets from the literature as well as sensitivity studies with the GEOS-Chem model. This model is a standard tool for investigation of tropospheric ozone [*Bey et al.*, 2001; *Martin et al.*, 2002; *X. Liu et al.*, 2006] and contributed to the *Stevenson et al.* [2006] model intercomparison. Results from a precursor version of GEOS-Chem [*Wang et al.*, 1998b] were reported in IPCC TAR (Table 2). As shown in Table 2, the global chemical production rates of ozone given by *Wang et al.* [1998b] were among the highest of the IPCC TAR models, whereas GEOS-Chem results are in the midrange of the post-2000 models and among the lowest of the *Stevenson et al.* [2006] intercomparison. As discussed below, this evolution reflects in part GEOS-Chem but more strongly the general model population.

[5] Part of our work in the present paper entails examining the sensitivity of the GEOS-Chem ozone budgets to the driving meteorological fields. GEOS-Chem was originally designed to use assimilated meteorological data from the Goddard Earth Observation System (GEOS) of the NASA Global Modeling and Assimilation Office (GMAO). We have recently developed the capability to drive GEOS-Chem with meteorological fields from the NASA/GISS general circulation model (GCM) for the purpose of studying the sensitivity of ozone and aerosol air quality to climate change. We will present here a comparative analysis of GEOS-Chem results driven by present-climate GISS GCM fields versus by the successive-generation GEOS-3 and GEOS-4 products at GMAO.

2. GEOS-Chem Model Driven by GISS Versus GEOS Meteorological Fields

[6] The tropospheric ozone simulation in GEOS-Chem was initially described by *Bey et al.* [2001], with significant updates presented by *Martin et al.* [2002, 2003a, 2003b], *Park et al.* [2004a] and *Evans and Jacob* [2005]. We use here GEOS-Chem version 7.02.04, which includes a fully coupled treatment of tropospheric ozone-NO_x-VOC chemistry and aerosols (http://www.as.harvard.edu/chemistry/trop/geos/). Cross-tropopause transport of ozone is represented by the Synoz flux boundary condition [*McLinden et al.*, 2000] with an imposed global annual mean STE flux of 510–540 Tg yr^{-1} (this variability reflects year-to-year differences in the model circulation). The STE fluxes for NO_x and total reactive nitrogen oxides (NO_y) are 0.4 and 2.3 Tg yr^{-1} respectively.

[7] Table 3 lists the global emissions of ozone precursors used in the present work. Anthropogenic emissions are for 1995. Biomass burning emissions are climatological means [*Duncan et al.*, 2003]. Lightning and biogenic emissions are computed locally within the model on the basis of meteorological variables, but are scaled to the same global totals in all simulations for the purpose of intercomparison. The scaling factors are globally uniform and determined by preliminary model runs calculating the unconstrained natural emissions. Lightning NO_x emissions are parameterized as a function of deep convective cloud top [*Price and Rind*, 1992; *Wang et al.*, 1998a; *Li et al.*, 2005] and are distributed vertically following *Pickering et al.* [1998]. Further details on the emission inventories are given by *Bey et al.* [2001].

[8] We present here results from GEOS-Chem driven by GEOS-3 and GEOS-4 meteorological fields (two successive versions of the GMAO assimilated product) for the same meteorological year (2001). The GEOS-3 and GEOS-4 products have 6-hour temporal resolution (3-hour for surface quantities and mixing depths), a horizontal resolution of 1° × 1° (GEOS-3) or 1° × 1.25° (GEOS-4), and 48 (GEOS-3) or 55 (GEOS-4) vertical layers. Winds are instantaneous variables in GEOS-3 and 6-hour averages in GEOS-4. More details about the GEOS-3 and GEOS-4 products can be found athttp://www.as.harvard.edu/chemistry/trop/geos/doc/man/gc_a4.html. For the simulations presented here, we use a horizontal resolution of 4° × 5° by spatial averaging of the meteorological fields.

[9] We also present results from GEOS-Chem driven by meteorological fields from the GISS GCM III, which is an updated version of the model used by *Rind et al.* [1999]. This GCM has a resolution of 4° × 5° with 23 layers in the vertical extending from the surface to 0.002 hPa (~85 km

altitude). We use archived GCM data for input to GEOS-Chem with the same temporal resolution as the GEOS data, i.e., 6-hour averages of winds, convective mass fluxes, temperature, humidity, cloud optical depths, and cloud fractions; and 3-hour averages of mixing depths and surface variables (precipitation, winds, temperature, albedo, solar radiation).

[10] A major difference between the GEOS-3, GEOS-4, and GISS models is the treatment of wet convection. GEOS-3 uses the Relaxed Arakawa-Schubert convection scheme [*Moorthi and Suarez*, 1992]. GEOS-4 has separate treatments of deep and shallow convection following the schemes developed by *Zhang and McFarlane* [1995] and *Hack* [1994]. The convection scheme in the GISS GCM was described by *Del Genio and Yao* [1993]. Unlike the GEOS models, the GISS GCM allows for condensed water in the atmosphere (i.e., condensed water is not immediately precipitated), resulting in frequent nonprecipitating shallow convection. In the wet deposition scheme, we do not scavenge soluble species from shallow convective updrafts at altitudes lower than 700 hPa in the GISS-driven model, whereas we do in the GEOS-driven model [*Liu et al.*, 2001]. The treatment of boundary layer turbulence is also different in GEOS and GISS. The mixing depth in GEOS is estimated from the bulk Richardson number with surface friction [*Holtslag and Boville*, 1993] and in the GISS GCM it is estimated on the basis of the vertical profile of turbulent kinetic energy [*Canuto*, 1994; *Canuto et al.*, 2001]. In either case, GEOS-Chem assumes instantaneous vertical mixing from the surface through the mixing depth [*Bey et al.*, 2001].

3. Sensitivity to Meteorological Fields

[11] A number of previous studies have evaluated GEOS-Chem simulations for ozone and its precursors using GEOS-3 and earlier-generation meteorological data products from GMAO [e.g., *Bey et al.*, 2001; *Martin et al.*, 2002; *Liu et al.*, 2004]. No such evaluations have been reported for GEOS-Chem driven by GEOS-4 or GISS products, and we compare those here to the GEOS-3 driven simulation. Both GEOS-3 and GEOS-4 simulations are for 2001. The GISS simulation is for 3 successive years of the present-day climate; interannual differences are small (Table 2 gives interannual ranges for global ozone budgets) and all results presented from the GISS simulation refer to the 3-year averages unless otherwise specified.

[12] Figure 1 shows the afternoon (1200–1600 local time) surface ozone concentrations simulated by GISS, GEOS-3 and GEOS-4 for January and July. Compared to GEOS-3 and GEOS-4, GISS produces higher levels of surface ozone, by up to 20% at high latitudes in winter. This appears to be largely driven by higher mixing depths and excessive high-latitude STE (D. Rind et al., Factors influencing tracer transport in GCMs, submitted to *Journal of Geophysical Research*, 2006).

[13] Zonal mean concentrations of NO_x, ozone, PAN, CO, and OH for January and July are compared in Figures 2a and 2b. Also shown is the rate constant $J_{O_3/^1D}$ for photolysis of O_3 to $O(^1D)$. The most prominent difference is in the simulated wintertime concentrations of PAN in the Northern Hemisphere, which are 30–40% higher in GISS than in GEOS-3 and GEOS-4. This is largely due to the colder temperatures in GISS, suppressing decomposition of PAN. There are also significant differences in the simulated OH and $J_{O_3/^1D}$ distributions, which appear to be due largely to differences in clouds (Figure 3). A previous GEOS-Chem study by *H. Liu et al.* [2006] and H. Liu et al. (Radiative effect of clouds on tropospheric chemistry: Sensitivity to cloud vertical distributions and optical properties, manuscript in preparation, 2007) found that the radiative impact of clouds on global OH in July (calculated from comparison of simulations with versus without clouds) is less than 1% for GEOS-3 but yields a 14% increase in OH for GEOS-4; we find an 18% increase in OH for GISS when the radiative effect of clouds is accounted for. GEOS-3 has compensating radiative effects from low clouds (enhancing OH above cloud) and high clouds (depleting OH below cloud), while GEOS-4 has much weaker clouds in the tropical middle and upper troposphere and GISS has thicker clouds in the tropical lower troposphere (Figure 3).

[14] Figures 4a and 4b compares the vertical profiles of simulated ozone to an ozonesonde data climatology [*Logan*, 1999] (with updates) at stations representative of different latitudinal bands. All three models reproduce observed ozone usually to within 10 ppb and with consistent gradients. The GISS model ozone is too high in the Arctic, particularly in winter because of excessive seasonal STE.

[15] Global budgets of tropospheric ozone for GEOS-Chem driven by GEOS-3, GEOS-4, and GISS meteorological fields are compared in Table 2. Production rates are 4250 Tg yr^{-1} in GEOS-3, 4470 Tg yr^{-1} in GISS, and 4700 Tg yr^{-1} in GEOS-4. Stronger photochemical activity in GEOS-4 is also reflected in a shorter ozone lifetime, so that the global ozone burdens in GEOS-3 and GEOS-4 are almost identical. The ozone burden in GISS is 7% higher than in GEOS-3 or GEOS-4, for reasons discussed above.

[16] Detailed accounting of the meteorological factors responsible for the differences in global ozone budgets between GEOS-3, GEOS-4, and GISS is difficult, but we identified three important factors. First is clouds, as discussed previously in the context of OH and $J(O^1D)$. Second is deep convective vertical mixing, which is stronger in GEOS-4 and GISS than in GEOS-3 and stimulates both ozone production and loss [*Lawrence et al.*, 2003]. Third is the distribution of lightning; GEOS-4 releases 45% of lightning NO_x in the Southern Hemisphere, where the ozone production efficiency per unit NO_x (OPE) is higher than in the Northern Hemisphere because of lower background NO_x [*Wang et al.*, 1998b], while that fraction is only 36% in GEOS-3.

[17] The global mass-weighted tropospheric concentration of OH in the GISS model is 1.08×10^6 molecules cm^{-3} on an annual mean basis, which is 5% higher than GEOS-3 (1.03×10^6 molecules cm^{-3}) and 4% lower than GEOS-4 (1.12×10^6 molecules cm^{-3}). The 3 year GISS simulation shows less than 1% interannual variability. These values are all consistent with the values derived by *Krol et al.* [1998] ($1.07^{+0.09}_{-0.17} \times 10^6$ molecules cm^{-3}) and *Spivakovsky et al.* [2000] (1.16 ± 0.17 molecules cm^{-3}). The lifetime of methane against oxidation by tropospheric OH ranges from 9.8 years in GEOS-4 to 11.1 years in GEOS-3, all consistent with the value of 9.1 ± 2.3 years derived from the global model studies reported in IPCC TAR [*Prather et al.*, 2001,

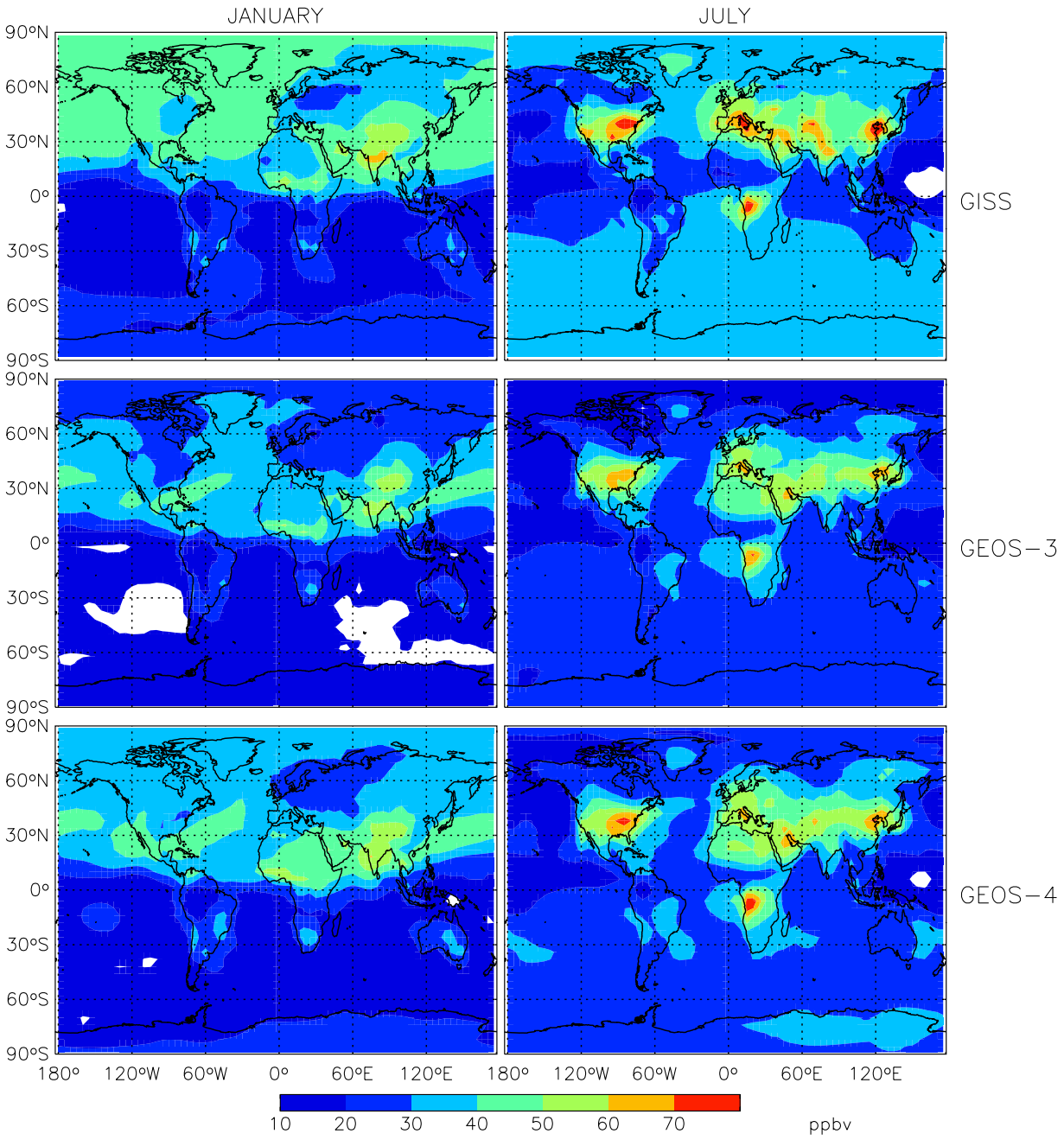

Figure 1. Ozone concentrations in afternoon surface air simulated by the GISS, GEOS-3, and GEOS-4 models in January and July. Values are monthly means for 1200–1600 local time.

Table 4.3] and the value of $10.2^{+0.9}_{-0.7}$ years derived by *Prinn et al.* [2005].

4. Ozone Budget Evolution Over the GEOS-Chem Model History

[18] The evolution of the global tropospheric production rate of ozone, $P(Ox)$, over the history of the GEOS-Chem model lends insight into the effects of different model developments. The GEOS-Chem precursor models by *Wang et al.* [1998a, 1998b] and *Mickley et al.* [1999] had $P(Ox)$ values of 4100 and 4330 Tg yr^{-1}. The first GEOS-Chem model version in the literature (version 3.02) [*Bey et al.*, 2001] calculated a higher $P(O_x)$ of 4900 Tg yr^{-1}, because of (1) better representation of cloud effects on UV actinic fluxes through the use of the fast-J algorithm [*Wild et al.*, 2000], (2) removal of a default absorbing aerosol layer with optical depth of 0.1 at 310 nm, and (3) higher NO_x emissions (45.6 Tg N yr^{-1} versus 42 Tg N yr^{-1} in the work by *Wang et al.* [1998a] and 40 Tg N yr^{-1} in the work by *Mickley et al.* [1999]), reflecting the use of 1994 versus 1985 anthropogenic inventories. *Martin et al.* [2002] used version 4.11 as a base for additional updates that included (1) reducing biomass burning NO_x emission from 12 to 6 Tg N yr^{-1}, which decreased $P(O_x)$ to 4760 Tg yr^{-1}; (2) accounting for the radiative and heterogeneous chemical effects of mineral dust, which further decreased $P(O_x)$ to 4440 Tg yr^{-1}; and (3) increasing lightning NO_x emission

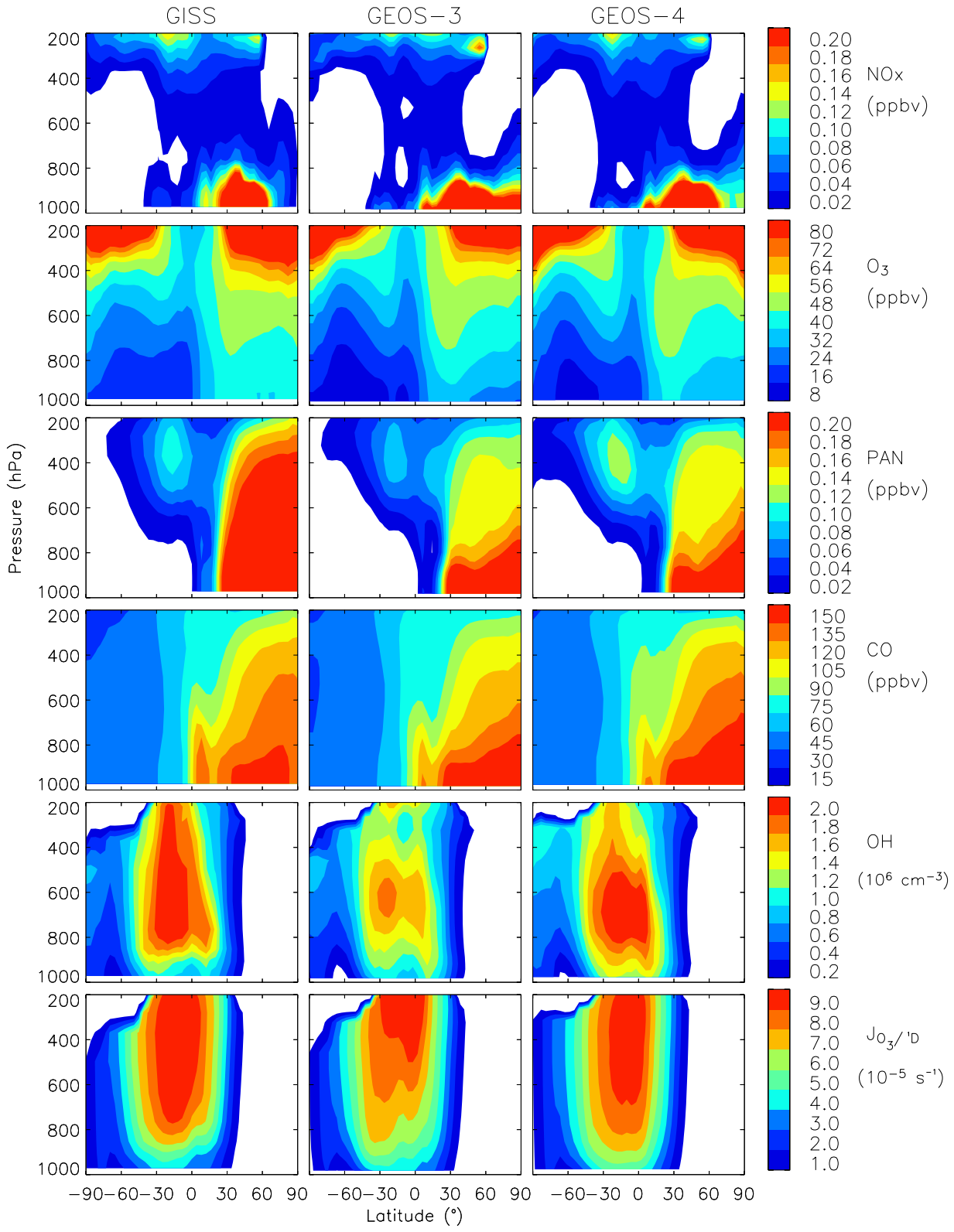

Figure 2a. January zonal mean concentrations of NO_x, ozone, PAN, CO, OH, and rate constant $J_{O_3/^1D}$ for photolysis of O_3 to $O(^1D)$, as simulated by the GISS, GEOS-3 and GEOS-4 models.

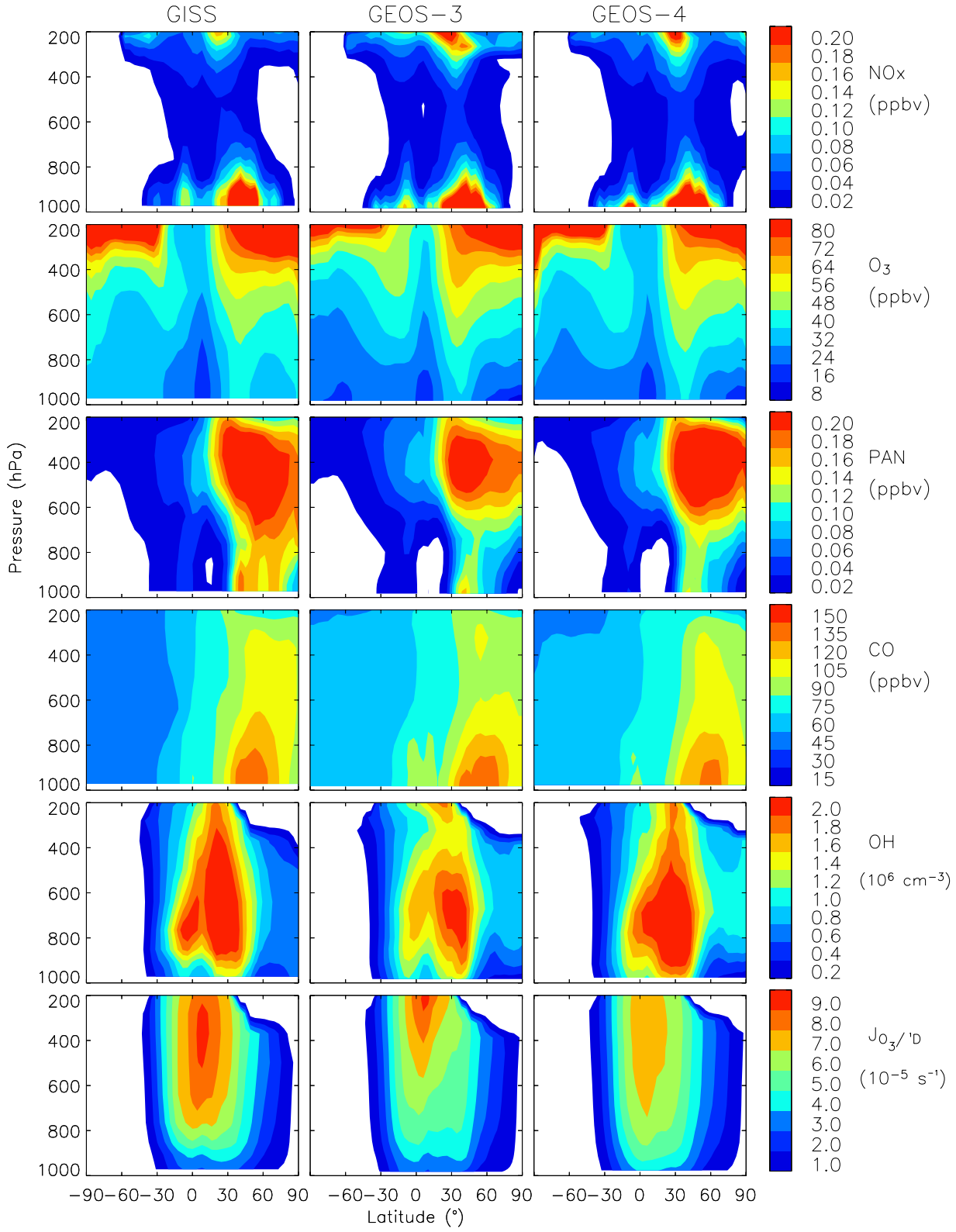

Figure 2b. Same as Figure 2a but for July.

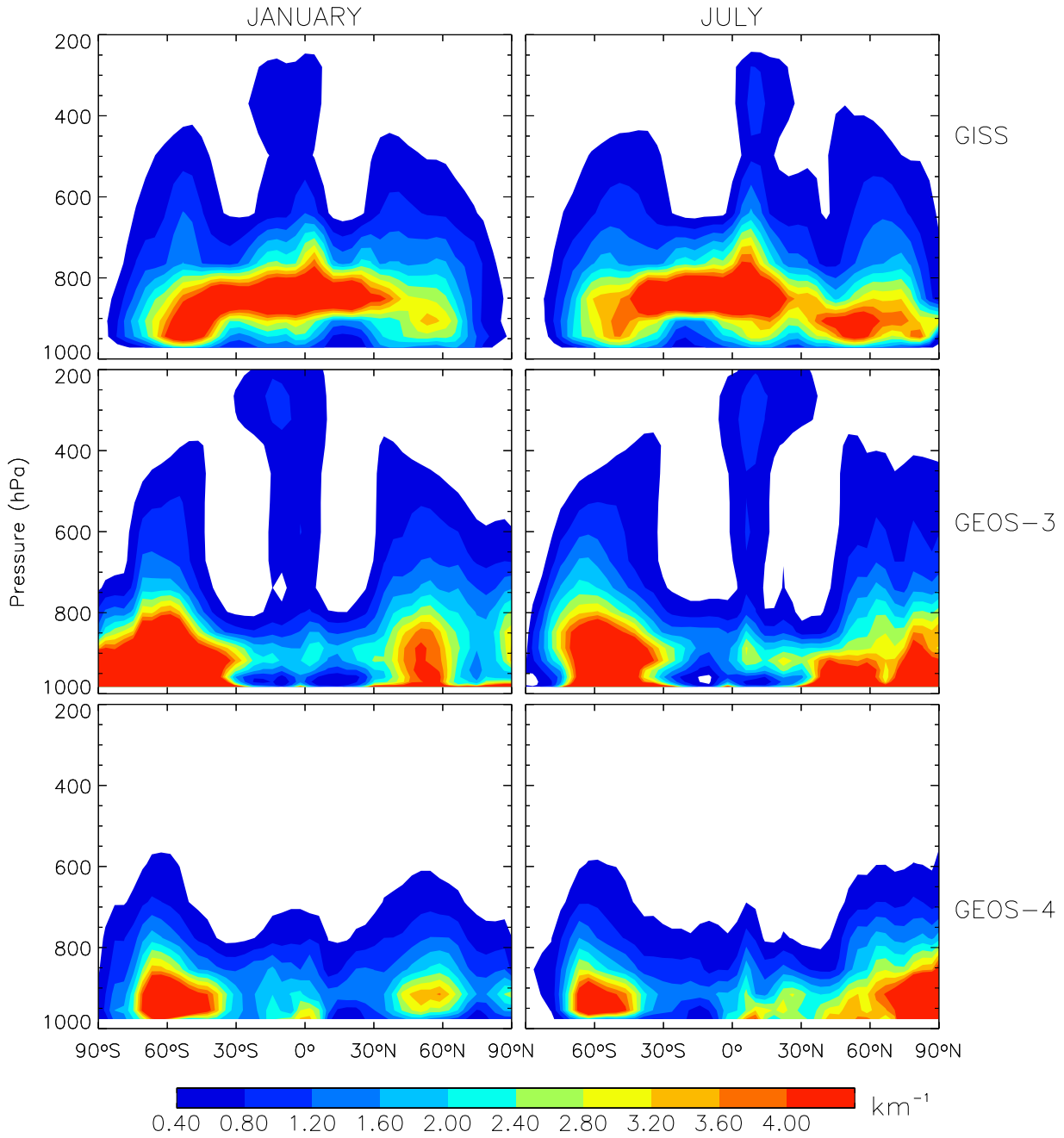

Figure 3. Zonal mean cloud extinction coefficients (km^{-1}) for the GISS, GEOS-3, and GEOS-4 models. Values are monthly means for January and July.

from 3 to 6 Tg N yr^{-1}, which increased $P(O_x)$ back to 4920 Tg yr^{-1}.

[19] Starting with version 4.13 (January 2001), a benchmarking process has been in place in which successive standard versions of GEOS-Chem are tested and documented with 1-month simulations for July, always starting from the same initial conditions. Figure 5 shows a 5-year history of the temporal evolution of $P(O_x)$ in these 1-month benchmarks. Details on each version are at http://www.as.harvard.edu/chemistry/trop/geos/geos_versions.html. $P(O_x)$ decreased from version 4.17 to 4.22 because of accounting of heterogeneous chemistry on mineral dust. The increase from version 4.22 to 4.23 reflects the doubling of lightning NO_x emission from 3 to 6 Tg N yr^{-1} to better reproduce observed ozone concentrations in the tropics [*Martin et al.*, 2002]. The decrease from version 4.26 to 4.27 is due to increase in the yield of organic nitrates from isoprene oxidation (hereinafter, isoprene nitrates), from 4% [*Chen et al.*, 1998] to 12% [*Sprengnether et al.*, 2002]. The peroxy radicals produced from oxidation of NMVOCs by OH react with NO by two branches:

(R1a) $RO_2 + NO \rightarrow RO + NO_2$

(R1b) $RO_2 + NO + M \rightarrow RONO_2 + M$

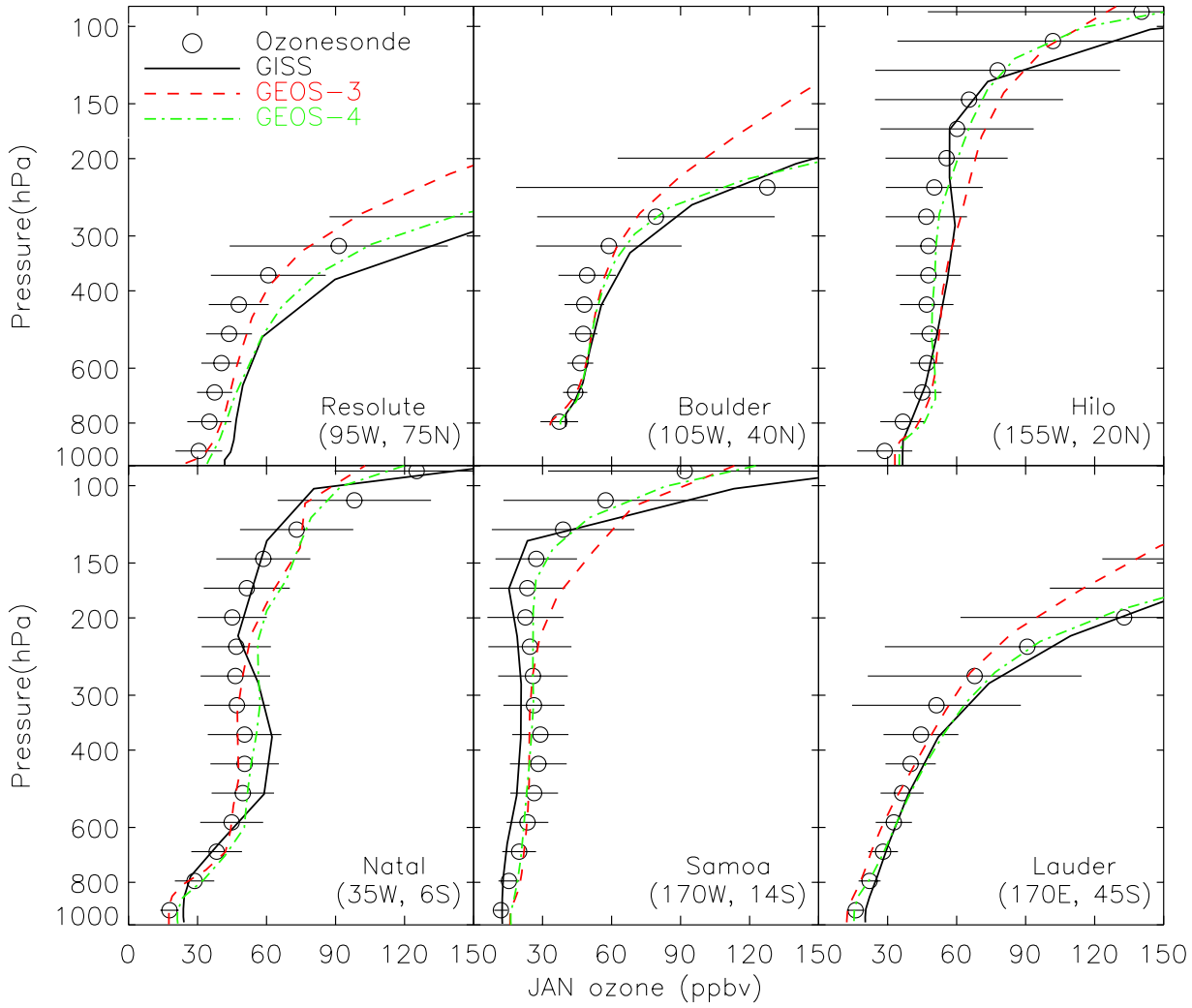

Figure 4a. Comparison of January monthly mean O_3 vertical profiles simulated by GISS (black solid lines), GEOS-3 (red dashed lines) and GEOS-4 (green dash-dotted lines) to climatological ozonesonde observations from *Logan* [1999] (open circles with horizontal bars for interannual standard deviation).

(R1a) results in O_3 production via subsequent NO_2 photolysis while (R1b) is a sink for NO_x by organic nitrate formation. The branching ratio (R1b)/(R1a) is determined by the number of carbon atoms in RO_2 and by temperature [*Atkinson*, 1990]. Isoprene nitrates have a hydroxy group that greatly enhances their water solubility, and we assume in GEOS-Chem that they are removed from the atmosphere by wet and dry deposition [*Chen et al.*, 1998; *Horowitz et al.*, 1998; *Liang et al.*, 1998; *Giacopelli et al.*, 2005; *Fiore et al.*, 2005].

[20] $P(O_x)$ slowly decreased from version 4.32 to 5.07.06 because of a succession of minor changes including the dry deposition of N_2O_5. The increase from version 5.07.06 to 5.07.07 resulted from the decrease in the N_2O_5 reaction probability ($\gamma_{N_2O_5}$) from a constant value of 0.1 to a value dependent on local aerosol composition with a global mean of 0.02 [*Evans and Jacob*, 2005]. The increase from version 6.02.02 to 6.02.03 is mainly due to reduced dust loadings associated with an updated dust mobilization scheme [*Zender et al.*, 2003; *Fairlie et al.*, 2007].

5. Variation Across Models in Global Tropospheric Ozone Budgets

5.1. Factors of Variability

[21] We now examine the variability in tropospheric ozone budgets for the ensemble of models reported in the literature. Values of $P(O_x)$ vary from 2300 to 4300 Tg yr^{-1} in the 1996–2000 literature reviewed by IPCC TAR and from 3300 to 5300 Tg yr^{-1} in the post-2000 literature compiled in Table 1. Compared to the older generation of models compiled in IPCC TAR, the ensemble of post-2000 models shows significant mean differences in global ozone budgets, including a 35% increase of ozone production, a 34% decrease of STE ozone flux, and a 10% increase of ozone burden (Table 2). The recent intercomparison of 21 current-generation models (including different versions

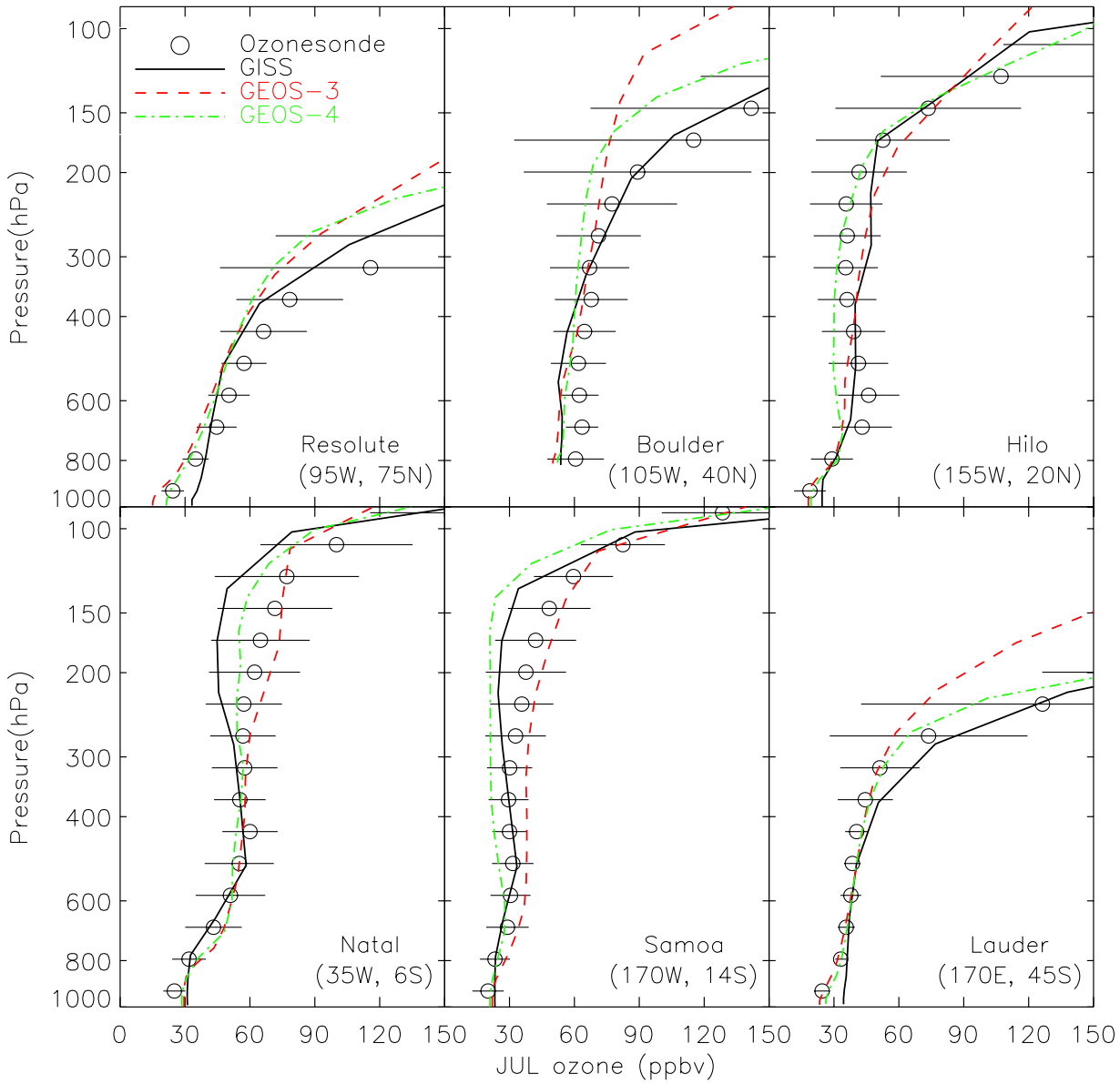

Figure 4b. Same as Figure 4a but for July.

of the same models) by *Stevenson et al.* [2006] shows a 10% further increase in mean $P(O_x)$ relative to the post-2000 literature (Table 2). All models in that intercomparison were constrained to use the same ozone precursor emissions from anthropogenic sources and biomass burning, while natural emissions were allowed to vary from model to model.

[22] The definitions for the tropopause and for the odd oxygen family (O_x) used to compute tropospheric ozone budgets may vary from one model to another, and this is a factor of variability in the budgets in Table 2. Most model studies use the thermal tropopause as determined by the temperature lapse rate, while some use a chemical tropopause ($[O_3]$ = 150 ppb) [e.g., *Prather et al.*, 2001; *Stevenson et al.*, 2004, 2006]. *Logan* [1999] showed from ozonesonde data that the mixing ratio of ozone is usually less than 150 ppbv at the thermal tropopause, except in summer at middle and high latitudes. We find in GEOS-Chem that the tropospheric ozone burden is 10% higher if we use the chemical versus thermal tropopause definition. *Stevenson et al.* [2004] previously found that $P(O_x)$ is relatively insensitive to the definition of the tropopause but that the ozone burden and lifetime are more affected. Some model budgets include peroxyacetylnitrates (PANs) and HNO_3 in their definition of the O_x family, while others do not, but this has little importance since peroxy radicals + NO reactions are the main contributors to $P(O_x)$ and are included in all models [*Stevenson et al.*, 1997; *Wauben et al.*, 1998; *Wang et al.*, 1998a; *Crutzen et al.*, 1999]. We find in our model that excluding PANs and HNO_3 from the O_x family causes a 10% increase in $P(O_x)$. These effects are relatively small, and there is no trend in their use that could explain the mean difference in budgets between the IPCC TAR and post-2000 models.

[23] The STE ozone fluxes in the older IPCC TAR models ranged from 390 to 1440 with a mean of 770 ±

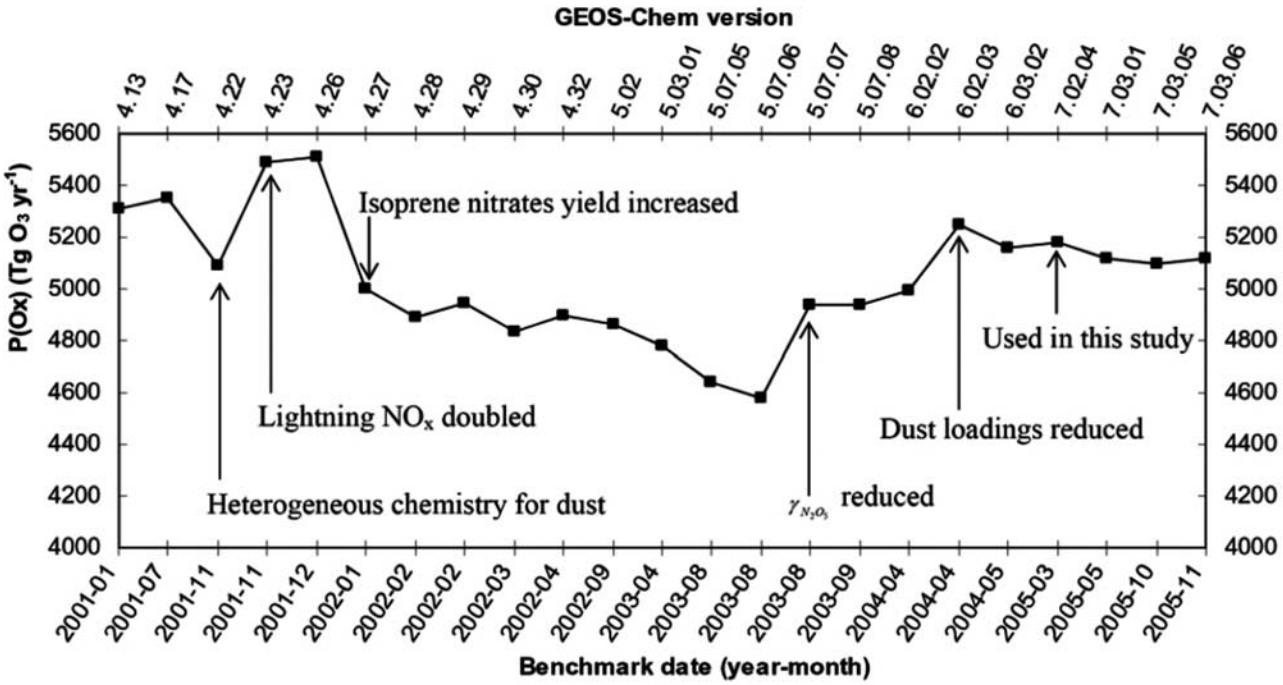

Figure 5. Evolution of global tropospheric ozone production $P(O_x)$ in the GEOS-Chem model since January 2001 (version 4.13). Values are from a 1-month benchmark in July, all with the same initial conditions, and are expressed in equivalent Tg yr^{-1} units; they are internally consistent but should not be compared to the full-year model values (Table 2) because of the effect of initial conditions and because $P(O_x)$ in July is higher than the annual mean.

400 Tg yr^{-1}. It is now recognized that many of these fluxes were too high, driven by artifacts in the vertical winds at the tropopause, particularly when using assimilated meteorological fields [*Tan et al.*, 2004; *van Noije et al.*, 2004]. Robust constraints from observed NO_y-N_2O-O_3 correlations in the lower stratosphere impose an STE ozone flux of 540 ± 140 Tg yr^{-1} [*Murphy and Fahey*, 1994; *Olsen et al.*, 2001]. The STE ozone flux in the current generation of global models in Table 2 (510 ± 90 Tg yr^{-1}) reflects that constraint, often through the use of a flux boundary condition (as in GEOS-Chem) or by relaxation to observed ozone concentrations above the tropopause region [*Horowitz et al.*, 2003].

[24] The lower STE ozone flux in the newer models leads to stronger tropospheric ozone production by reducing the NO_2/NO concentration ratio in the upper troposphere. We conducted a sensitivity study using our GISS-driven GEOS-Chem simulation with the STE ozone flux increased by 25% to 625 Tg yr^{-1} (Table 4). The 25% increase resulted in a 5% increase of O_3 burden, a 3% increase of O_3 lifetime, and a 1% decrease of $P(O_x)$. The increase in $P(O_x)$ between the IPCC TAR models and more recent ones is much larger, and the trend in O_3 burden is positive, so this cannot be a dominant effect.

[25] Tropospheric ozone production is highly sensitive to the supply of NO_x. *Stevenson et al.* [2006] pointed out that the higher NO_x and isoprene emissions used in their model intercomparison study were two important factors for their much higher ozone production rates compared to IPCC TAR values, with each factor accounting for about half of the increase of $P(O_x)$ in one specific model (FRSGC/UCI). Comparison of the older global models compiled by IPCC TAR [*Prather et al.*, 2001] versus the post-2000 literature of Table 1 shows a mean increase across models in global surface NO_x emission (excluding lightning and aircraft) from 34.9 to 38.8 Tg N yr^{-1}, and an increase in lightning

Table 4. GEOS-Chem Model Sensitivities of Global Tropospheric Ozone and OH Budgets[a]

	Chemical Production Rate of Ozone, Tg yr^{-1}	Chemical Loss Rate of Ozone, Tg yr^{-1}	Ozone Burden, Tg	Ozone Lifetime, days	OH, 1×10^6 molecules cm^{-3}	Methane Lifetime, years
Standard simulation[b]	4487	3999	319	23.3	1.08	10.6
STE +25%	4445	4065	335	24.1	1.08	10.5
Fossil fuel NO_x emission +25%	4649	4113	325	23.0	1.11	10.3
Lightning NO_x emission +25%	4672	4158	328	23.2	1.14	10.1
Isoprene emission −25%	4486	3991	319	23.4	1.13	10.1
No isoprene emission	4394	3900	315	23.5	1.28	8.8
No NMVOCs emissions	3986	3566	298	24.3	1.31	8.7

[a]All simulations are for 1 year (with 6-month initialization) driven by the same GISS meteorology.

[b]Standard simulation as presented in the text including stratosphere-troposphere exchange (STE) of 500 Tg yr^{-1}, NO_x emission from fossil fuel combustion of 23.6 Tg N yr^{-1}, lightning NO_x emission of 4.7 Tg N yr^{-1}, and isoprene emission of 400 Tg C yr^{-1} (Table 3). All sensitivity simulations are relative to the standard simulation.

Table 5. Global Model Parameters for the Present-Day Atmosphere Used in the $P(O_x)$ Regression Analysis[a]

Reference	Model	E_{NOx}, Tg N yr^{-1}		E_{NMVOC}, Tg C yr^{-1}	STE, Tg yr^{-1}	P(O_x), Tg yr^{-1}
		Surface	Lightning			
Roelofs and Lelieveld [1997]	ECHAM	33	4	0	460	3430
Hauglustaine et al. [1998]	MOZART	36	5	650	390	3020
Houweling et al. [1998]	TM3	33	5	510	770	3980
Houweling et al. [1998][b]	TM3	33	5	0	740	2890
Wang et al. [1998b]	HARVARD	39	3	700	400	4100
Wauben et al. [1998]	KNMI	31	5	0	1430	2860
Crutzen et al. [1999]	MATCH	35	2	0	1440	2490
Lawrence et al. [1999]	MATCH-MPIC	35	2	0	1100	2330
Lelieveld and Dentener [2000]	TM3	38	5	530	570	3310
Stevenson et al. [2000]	STOCHEM	36	5	590	430	4320
Wild and Prather [2000]	UCI	38	5	600	470	4230
Bey et al. [2001]	GEOS-Chem	42	3	510	470	4900
Sudo et al. [2002]	CHASER	38	5	650	590	4900
Horowitz et al. [2003]	MOZART-2	42	3	750	340	5260
von Kuhlmann et al. [2003]	MATCH-MPIC	38	5	530	540	4560
Hauglustaine et al. [2004]	LMDz-INCA	42	5	0	520	4490
Stevenson et al. [2004]	STOCHEM	41	7	850	400	4980
Wild et al. [2004]	FRSGC/UCI	38	5	600	520	4090
Stevenson et al. [2006]	14 models	44 ± 1	6 ± 1	610 ± 200	590 ± 140	4970 ± 400

[a]Including all 32 models from the literature compiled in Tables 1 and 2 that provide information on NO_x emissions E_{NOx}, NMVOC emissions E_{NMVOC}, stratosphere-tropopause exchange fluxes STE, and ozone production rates $P(O_x)$. This includes 14 of the models participating in the *Stevenson et al.* [2006] intercomparison; these models are treated in the regression analysis as individual elements.

[b]Results from sensitivity study without NMVOCs.

NO_x emission from 4.0 to 4.9 Tg N yr^{-1} (Table 5). The former reflects an actual rise in Asian NO_x anthropogenic emissions between the ca. 1985 inventories used by the IPCC TAR models versus the early 1990s inventories used in the more recent models [*Fusco and Logan*, 2003]. There is large uncertainty associated with lightning NO_x emissions. State-of-science estimates range from 1 to 20 Tg N yr^{-1} [*Price et al.*, 1997; *Boersma et al.*, 2005], though global models use values in the range 2–7 Tg N yr^{-1} to reproduce observed ozone and NO_y concentrations in the tropics [e.g., *Levy et al.*, 1996; *Martin et al.*, 2002; *Tie et al.*, 2002; *Li et al.*, 2005].

[26] Another significant difference between the newer and older generation of global models is the treatment of NMVOCs. Only about half of the models compiled in IPCC TAR included NMVOC chemistry while almost all models in the post-2000 literature do. Isoprene from vegetation generally accounts for most of total NMVOC emissions (Table 3). *Houweling et al.* [1998] found in their model that $P(O_x)$ would decrease by 27% in the absence of NMVOCs. Subsequent model studies [*Roelofs and Lelieveld*, 2000; *Poisson et al.*, 2000; *von Kuhlmann et al.*, 2004] found a somewhat weaker effect, ranging from 16% to 24%. Changing methane would also have a major effect on global tropospheric ozone budgets [*Wang and Jacob*, 1998; *Fiore et al.*, 2002], but models simulating present-day conditions all use sensibly the same methane levels constrained by observations.

5.2. Regression Analysis for Global Ozone Production in Models

[27] To explore these issues further, we conducted a multivariate regression analysis of present-day $P(O_x)$ versus model parameters for the ensemble of 32 models compiled in Table 2 for which sufficient information was available. This included 18 models from the literature plus the 14 models from the *Stevenson et al.* [2006] intercomparison that reported a model STE (Table 5). We find that 74% of the variance of $P(O_x)$ across models can be explained by the global total NO_x emissions (E_{NOx}), STE, and NMVOC emissions (E_{NMVOC}) through the following regression ($R^2 = 0.74$, $n = 32$):

$$P(O_x) = 104\ E_{NOx} + 0.96\ E_{NMVOC} - 0.47\ STE - 581 \quad (1a)$$

where $P(O_x)$ and STE are in Tg yr^{-1}, E_{NOx} is in Tg N yr^{-1}, and E_{NMVOC} is in Tg C yr^{-1}. The 85% confidence intervals for the coefficients of E_{NOx}, E_{NMVOC} and STE are [73, 136], [0.48, 1.45] and [−0.93, −0.01] respectively.

[28] We also find that an alternative regression model with on/off dependence on NMVOC emissions can equally explain ($R^2 = 0.74$) the variation of $P(O_x)$ across models:

$$P(O_x) = 106\ E_{NOx} + 672\ \delta(NMVOC) - 0.40\ STE - 753 \quad (1b)$$

where $\delta(NMVOC)$ is 1 if NMVOCs are included in the model and 0 otherwise. The step dependence on NMVOCs will be discussed below. The success of equations (1a) and (1b) in reproducing the $P(O_x)$ for each of the 32 models included in the regression analysis is shown in Figures 6a and 6b. Differences are less than 500 Tg yr^{-1} for most of the models. Higher-order terms in the regression, including the product $E_{NOx}E_{NMVOC}$, did not improve the regression results.

[29] Applying equation (1a) to the values of E_{NOx}, E_{NMVOC}, and STE in the individual models yields a mean $P(O_x)$ increase of 870 Tg yr^{-1} from the IPCC TAR models to the post-2000 literature, which is 72% of the actual increase shown in Table 2 (1200 Tg yr^{-1}). Additive increases of 520, 230 and 120 Tg yr^{-1} result respectively from the increases of NO_x and NMVOC emissions and from the decrease of STE. The other 28% of the $P(O_x)$ increase may be due to other changes in models over the past decade including better parameterizations of convection [*Chatfield and Delany*, 1990; *Pickering et al.*, 1992;

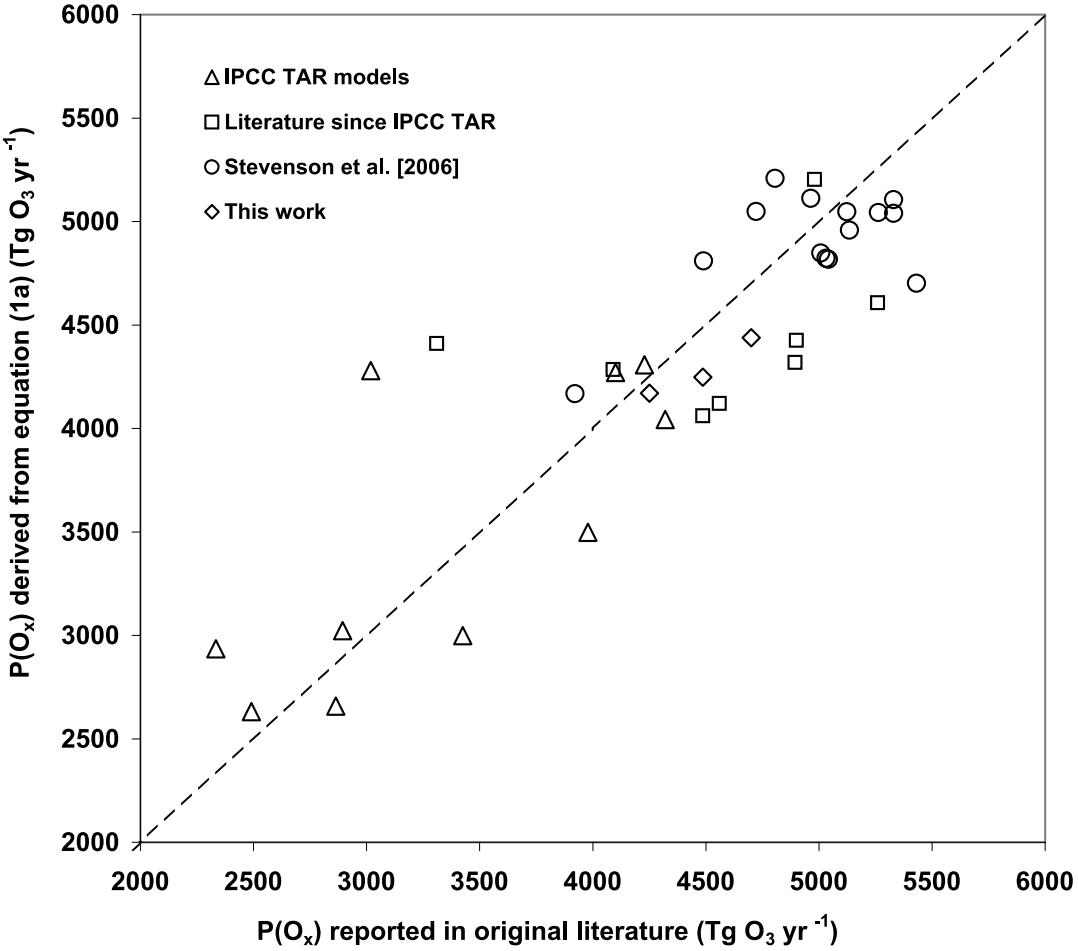

Figure 6a. Global ozone production rates from the 32 models in Table 5 as derived from the regression equation (1a) versus the actual values reported in the literature. Results from the three GEOS-Chem simulations presented in this work (driven by GEOS-3, GEOS-4, and GISS) are also plotted.

Horowitz et al., 2003], cloud radiative effects [*Wild et al.*, 2000], and aerosol extinction [*Martin et al.*, 2002; *Bian et al.*, 2003; *Tie et al.*, 2005], as well as equatorward shift of anthropogenic emissions [*Gupta et al.*, 1998; *Stevenson et al.*, 2006]. Similarly, 1510 Tg yr^{-1} or 89% of the actual increase (1690 Tg yr^{-1}, Table 2) of $P(O_x)$ in the work by *Stevenson et al.* [2006] relative to IPCC TAR models can be explained with equation (1a). Equation (1b) yields similar results. The higher $P(O_x)$ in the *Stevenson et al.* [2006] intercomparison relative to the ensemble mean of post-2000 models can be largely explained by higher NOx emissions.

5.3. Interpretation of the Regression Analysis

[30] We now offer a physical interpretation for the individual terms in the regression equation (1) that successfully describe global tropospheric ozone production in models. The coefficient of E_{NOx} represents the ozone production efficiency (OPE = $\partial P(O_x)/\partial E_{NOx}$), and is 30 mol mol^{-1} in (1a) and 31 mol mol^{-1} in (1b). Fossil fuel combustion accounts for about half of total NO_x emission in the models (Table 3). We conducted a sensitivity analysis in GEOS-Chem increasing the global NO_x emission from fossil fuel combustion by 25%, which raises E_{NOx} by 13% or 5.9 Tg N yr^{-1} (Table 4). We found that the global ozone production increased by 162 Tg yr^{-1}. The OPE derived from this perturbation (8 mol mol^{-1}) is much smaller than the OPE derived from equation (1). In a separate sensitivity test, we increased the global lightning NO_x emission by 25% (1.2 Tg N yr^{-1}, representing a 2.7% increase of E_{NOx}) and found that $P(O_x)$ increased by 185 Tg yr^{-1} (Table 4). The OPE derived from this perturbation (45 mol mol^{-1}) is much larger than the OPE derived from equation (1). Thus lightning NO_x is about 6 times more efficient in driving ozone production than anthropogenic NO_x. Separating lightning from other sources of NO_x in the linear regression (1) does not however produce a significantly higher correlation.

[31] The dependence of $P(O_x)$ on STE is expressed in equation (1) by a linear sensitivity coefficient $\partial P(O_x)/\partial STE$, which is -0.47 mol mol^{-1} in (1a) and -0.40 mol mol^{-1} in (1b). We find in GEOS-Chem that $P(O_x)$ decreases by 45 Tg $yr^{-1}$when we increase STE by 25% (Table 4), yielding a sensitivity coefficient of -0.36 mol mol^{-1} which is consistent with the result from the linear regression.

[32] Equations (1a) and (1b) can explain the differences of $P(O_x)$ across global models equally well but imply different sensitivities to E_{NMVOC}. Equation (1a) implies a linear dependence while (1b) implies a step dependence

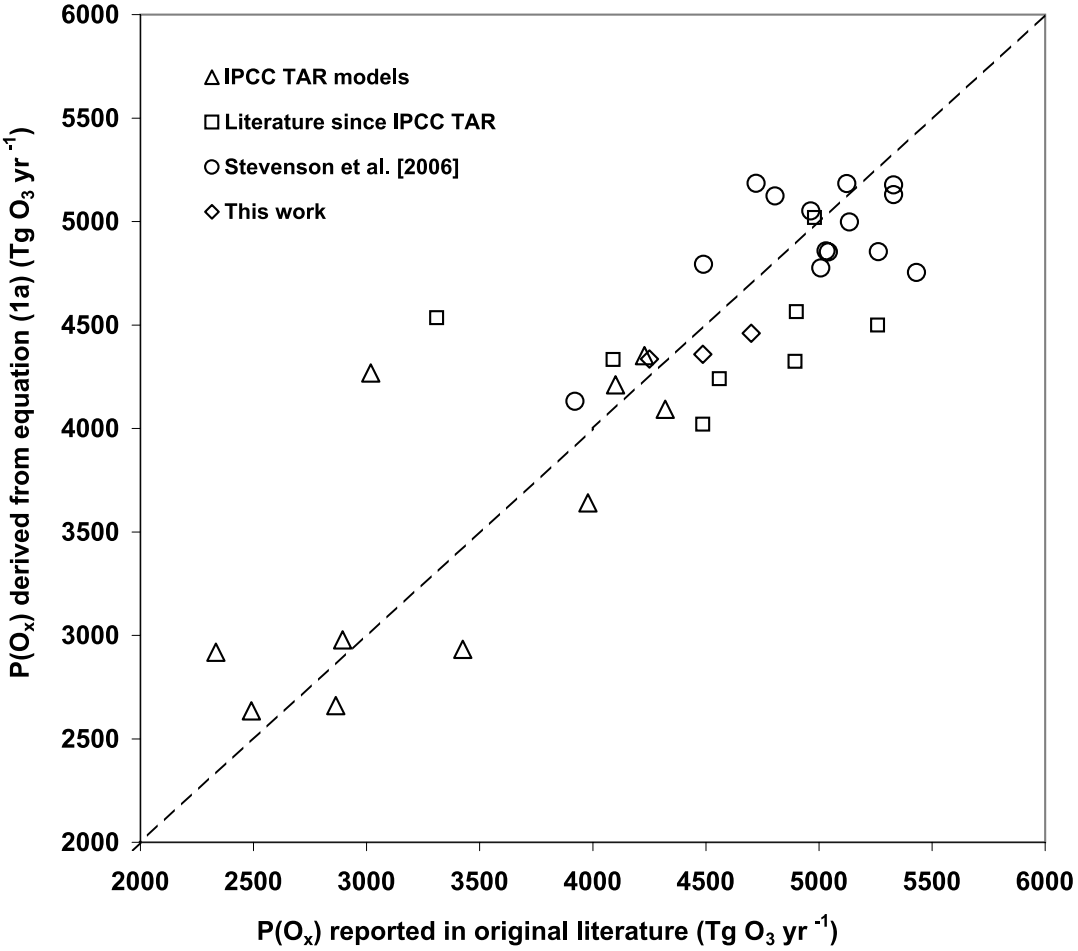

Figure 6b. Same as Figure 6a but the ozone production rates are derived from equation (1b) instead of (1a).

where $P(Ox)$ increases by 670 Tg yr^{-1} when NMVOC emissions are included but does not increase further within the typical range of 500–900 Tg C yr^{-1} used in models (isoprene being the dominant contributor).

[33] We conducted further analysis to reconcile the discrepancy between equations (1a) and (1b). Figure 7 shows the sensitivity of $P(O_x)$ to NMVOC emissions for the ensemble of models used in the regression analysis, after standardizing to the same values of STE (510 Tg yr^{-1}) and E_{NOx} (45 Tg N yr^{-1}) using equation (1a). We see that the models results can be classified into two groups, with versus without NMVOCs. Models with NMVOCs tend to have higher ozone production, with the exception of two outliers [*Hauglustaine et al.*, 1998; *Lelieveld and Dentener*, 2000]. Among the models including NMVOC chemistry, however, there is no clear dependence of $P(O_x)$ on NMVOC emission. Although it is well known from regional ozone models that ozone production is often NMVOC-saturated, this refers to the local ozone production rate [e.g., *Sillman et al.*, 1990], not to the ultimate ozone production as computed in a global model. Increasing NMVOCs would be expected to increase the OPE both by decreasing OH levels (and hence increasing the lifetime of NO_x) and by promoting the sequestration of NO_x as PAN and its eventual release in regions of high OPE [*Lin et al.*, 1988; *Houweling et al.*, 1998; *Wang et al.*, 1998c; *Poisson et al.*, 2000; *Roelofs and Lelieveld*, 2000; *Hudman et al.*, 2007; *von Kuhlmann et al.*, 2004].

[34] We conducted three GEOS-Chem sensitivity simulations with NMVOC emissions modified from the standard values in Table 3: one with isoprene emission reduced by 25%, one with isoprene emission set to zero, and one with all NMVOC emissions set to zero (Table 4). The sensitivity simulations show saturation (Figure 7) for NMVOC emissions greater than 200 Tg C yr^{-1}. We find that the saturation is due to the formation of organic nitrates, especially isoprene nitrates, providing a significant sink for NO_x as discussed in section 4. The importance of this sink for NO_x has been discussed in previous model studies [*Horowitz et al.*, 1998; *Liang et al.*, 1998; *von Kuhlmann et al.*, 2004; *Fiore et al.*, 2005]. As shown in Figure 8, increasing isoprene emissions in GEOS-Chem saturates PAN as well as ozone, while causing sharp decreases in NO_x and OH.

[35] Although it is most likely (as assumed in GEOS-Chem) that isoprene nitrate formation is a terminal sink for NO_x [*Giacopelli et al.*, 2005], some models recycle isoprene nitrate to NO_x through reaction with OH [*Grossenbacher et al.*, 2001] or do not include isoprene nitrate formation. Those models would have greater positive response of $P(O_x)$ to the magnitude of isoprene emissions [*Fiore et*

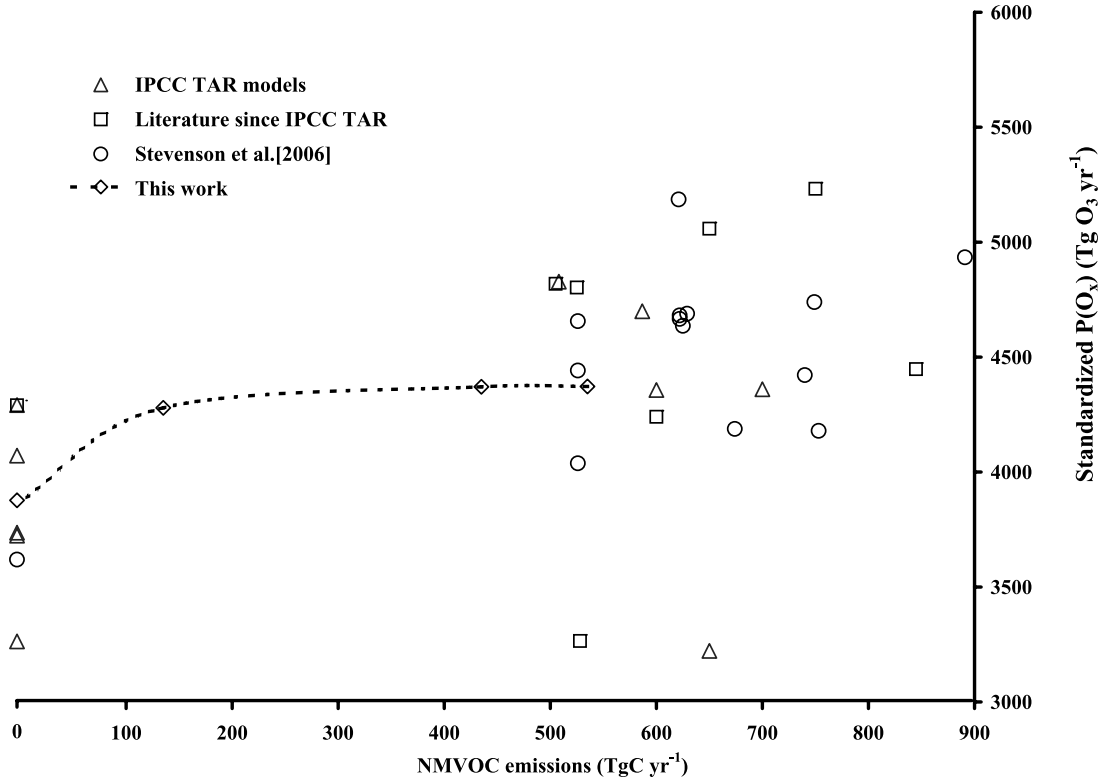

Figure 7. Sensitivity of global ozone production rate $P(O_x)$ to NMVOC emissions for the ensemble of models compiled in Table 5, and also including results from this study. The values of $P(O_x)$ from the original publications have been standardized to the same STE (510 Tg yr^{-1}) and E_{NOx} (45 Tg N yr^{-1}) using equation (1a). The dashed line shows results from GEOS-Chem sensitivity simulations (see text for details).

al., 2005]. We find in GEOS-Chem that $P(O_x)$ decreases by 11% in the absence of NMVOCs. This sensitivity is at the low end of values reported in the literature, e.g., 16% [*Roelofs and Lelieveld*, 2000], 22% [*von Kuhlmann et al.*, 2004], 22% [*Poisson et al.*, 2000], 27% [*Houweling et al.*, 1998]. *Roelofs and Lelieveld* [2000] viewed isoprene nitrate as a terminal NO_x sink, as we do here, while the other studies allowed it to recycle to NO_x.

[36] We find that the annual mean, mass-weighted tropospheric OH concentration in GEOS-Chem increases by 21% and the methane lifetime against oxidation by tropospheric OH decreases by 18% in the absence of NMVOCs. This sensitivity is at the high end of model results reported in literature: *Houweling et al.* [1998] found that including NMVOCs hardly affected the tropospheric OH burden; *Roelofs and Lelieveld* [2000] reported that tropospheric OH decreases by about 8% when NMVOCs are accounted for; *Poisson et al.* [2000] and *von Kuhlmann et al.* [2004] found that in the absence of NMVOCs the methane lifetime would decrease by 12% and 2%, respectively. Our higher sensitivity of OH to NMVOCs again appears to reflect the treatment of isoprene nitrate as a terminal sink for NO_x; NMVOCs not only provide a sink for OH but also for NO_x, further reducing OH levels.

6. Conclusions

[37] Global models of tropospheric ozone show large differences in their global ozone budget terms. The production rate $P(O_x)$ of ozone in the troposphere varies from 2300 to 5300 Tg yr^{-1} across models documented in the literature since 1996. The ensemble mean of $P(O_x)$ in post-2000 models has increased by 35% relative to the older generation compiled by the IPCC TAR. A recent 21-model intercomparison by *Stevenson et al.* [2006] reports even higher $P(O_x)$. Trends in the mean global burden of tropospheric ozone computed by these models have been much weaker, about 10%, reflecting compensating effects from weaker stratosphere-troposphere exchange (STE) and shorter ozone lifetimes. Better understanding of the factors driving the variability in $P(O_x)$ across models is important because of its implications for the computed sensitivity of tropospheric ozone to perturbations.

[38] We investigated this issue by using a global tropospheric chemistry model (GEOS-Chem) driven by three different sets of meteorological fields: assimilated data for 2001 (GEOS-3 and GEOS-4) and GISS GCM III present-day climate. The interface with GCM fields is a new development for GEOS-Chem designed to enable study of the effects of climate change on atmospheric composition. The GISS GCM fields provide a simulation of tropospheric ozone and its precursors that is consistent with the established GEOS-driven simulations. The simulated wintertime concentrations of PAN in the Northern Hemisphere in GISS are 30–40% higher than in GEOS-3 and GEOS-4, largely because of colder temperatures. The GISS simulation overestimates surface ozone by up to 20% over the high latitudes in winter, because of excessive STE at high latitudes.

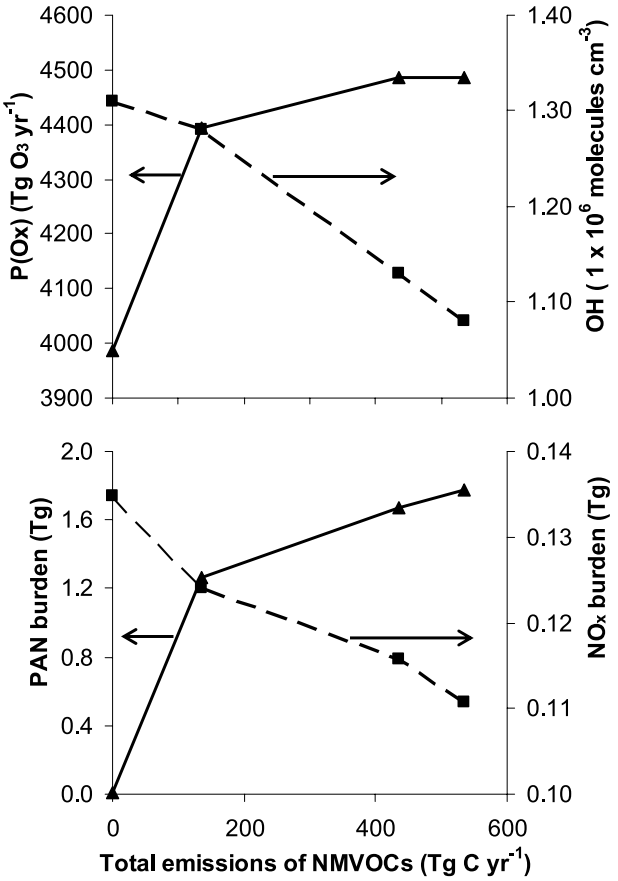

Figure 8. Sensitivity to NMVOC emissions of tropospheric ozone production $P(O_x)$, mass-weighted tropospheric OH concentration, and tropospheric PAN and NO_x burdens. Values are global annual means from GEOS-Chem sensitivity simulations.

[39] The $P(O_x)$ values in the GEOS-Chem model driven by the different meteorological fields vary from 4250 Tg yr^{-1} with GEOS-3 to 4700 Tg yr^{-1} with GEOS-4, with GISS yielding intermediate results. Different cloud distributions are the principal cause for these differences. Different distributions of lightning NO_x emissions (driven by deep convection) also contribute, even though the global lightning source is kept the same in all simulations. This sensitivity highlights, especially in the context of climate change, the importance of better describing cloud processes and lightning NO_x emissions in global models of tropospheric chemistry.

[40] Tropospheric ozone budgets in GEOS-Chem have seen little net change over the 5-year model history, in apparent contrast to the general population of models. We examined the historical evolution of tropospheric ozone budgets in GEOS-Chem by using archives of 1-month code benchmarks applied to successive model versions. We find major but eventually compensating effects over the model history from inclusion of radiative and chemical properties of dust, decrease in the N_2O_5 reaction probability for uptake by aerosols, increase in the lightning NO_x source, and increase in the isoprene nitrate formation yield.

[41] We further explored the causes of the variability of $P(O_x)$ across an ensemble of 32 global models reported in the literature for present-day conditions, by conducting a multivariate linear regression analysis of the variation of $P(O_x)$ with model parameters. Our results show that 74% of the variance of $P(O_x)$ across models can be explained by linear dependences on NO_x emissions, NMVOC emissions (mostly biogenic isoprene), and STE. An equally good statistical fit is obtained with a delta function for NMVOC emissions (1 when NMVOC chemistry is considered in the model and 0 otherwise). The latter implies a saturation of $P(O_x)$ with increasing NMVOCs. Either regression form can largely explain the 25% increase in the ensemble mean $P(O_x)$ for the post-2000 models relative to the IPCC TAR models. This increase is driven by higher NO_x emissions (15%), more widespread inclusion of NMVOC emissions (7%), and weaker STE (3%).

[42] Although $P(O_x)$ is sensitive to the inclusion of NMVOC chemistry in models, it does not appear generally sensitive to the magnitude of NMVOC emissions within the typical range used by the models (500–900 Tg C yr^{-1}). GEOS-Chem sensitivity simulations with variable NMVOC emissions show a saturation of $P(O_x)$ when emissions exceed 200 Tg C yr^{-1}. This saturation effect is due to the formation of isoprene nitrates, providing a significant sink for NO_x. Models that do not include isoprene nitrate formation or that allow the recycling of NO_x from isoprene nitrate would not show such a saturation effect.

[43] Our analysis of the factors determining the variability of $P(O_x)$ has been for the present-day atmosphere, with known levels of methane. For past or future atmospheres, changing methane needs to be accounted as an additional factor affecting the tropospheric ozone budget [*Wang and Jacob*, 1998; *Fiore et al.*, 2002]. This could be included as an additional linear term in the regression analysis (1); *Wang and Jacob* [1998] find an ozone production efficiency of 0.7 moles per mole of methane oxidized in a model perturbation to the preindustrial atmosphere, with little variation of this efficiency over a range of conditions. Unlike isoprene, oxidation of methane does not produce organic nitrates with significant yield.

[44] **Acknowledgments.** This research was supported by the Science to Achieve Results (STAR) program of the U.S. Environmental Protection Agency. Jennifer A. Logan was supported by NASA grant NNG05GG34G. We thank Arlene Fiore (NOAA/GFDL), Hongyu Liu (National Institute of Aerospace) and Oliver Wild (University of Cambridge) for valuable discussions.

References

Atkinson, R. (1990), Gas-phase tropospheric chemistry of organic compounds: A review, *Atmos. Environ.*, *24*, 1–41.

Bey, I., D. J. Jacob, R. M. Yantosca, J. A. Logan, B. D. Field, A. M. Fiore, Q. Li, H. Y. Liu, L. J. Mickley, and M. G. Schultz (2001), Global modeling of tropospheric chemistry with assimilated meteorology: Model description and evaluation, *J. Geophys. Res.*, *106*, 23,073–23,095.

Bian, H., M. J. Prather, and T. Takemura (2003), Tropospheric aerosol impacts on trace gas budgets through photolysis, *J. Geophys. Res.*, *108*(D8), 4242, doi:10.1029/2002JD002743.

Boersma, K. F., H. J. Eskes, E. W. Meijer, and H. M. Kelder (2005), Estimates of lightning NO_x production from GOME satellite observations, *Atmos. Chem. Phys.*, *5*, 2311–2331.

Canuto, V. M. (1994), Large-eddy simulation of turbulence: A subgrid scale model including shear, vorticity, rotation and buoyancy, *Astrophys. J.*, *428*, 729–752.

Canuto, V. M., A. Howard, Y. Cheng, and M. S. Dubovikov (2001), Ocean turbulence, part I: One-point closure model—Momentum and heat vertical diffusivities, *J. Phys. Ocean.*, *31*, 1413–1426.

Chatfield, R. B., and A. C. Delany (1990), Convection links biomass burning to increased tropical ozone: However, models will tend to overpredict O_3, *J. Geophys. Res.*, *95*(D11), 18,473–18,488.

Chen, X., D. Hulbert, and P. B. Shepson (1998), Measurement of the organic nitrate yield from OH reaction with isoprene, *J. Geophys. Res.*, *103*, 25,563–25,568.

Crutzen, P. J., et al. (1999), On the background photochemistry of tropospheric ozone, *Tellus, Ser. A-B*, *51*, 123–146.

Del Genio, A. D., and M. Yao (1993), Efficient cumulus parameterization for long-term climate studies: The GISS scheme, in *The Representation of Cumulus Convection in Numerical Models*, *Meteorol. Monogr.*, *46*, 181–184.

Duncan, B. N., R. V. Martin, A. C. Staudt, R. Yevich, and J. A. Logan (2003), Interannual and seasonal variability of biomass burning emissions constrained by satellite observations, *J. Geophys. Res.*, *108*(D2), 4100, doi:10.1029/2002JD002378.

Evans, M. J., and D. J. Jacob (2005), Impact of new laboratory studies of N_2O_5 hydrolysis on global model budgets of tropospheric nitrogen oxides, ozone, and OH, *Geophys. Res. Lett.*, *32*, L09813, doi:10.1029/2005GL022469.

Fairlie, T. D., D. J. Jacob, and R. J. Park (2007), The impact of transpacific transport of mineral dust in the United States, *Atmos. Environ.*, *41*, 1251–1266.

Fiore, A. M., D. J. Jacob, B. D. Field, D. G. Streets, S. D. Fernandes, and C. Jang (2002), Linking ozone pollution and climate change: The case for controlling methane, *Geophys. Res. Lett.*, *29*(19), 1919, doi:10.1029/2002GL015601.

Fiore, A. M., L. W. Horowitz, D. W. Purves, H. Levy II, M. J. Evans, Y. Wang, Q. Li, and R. M. Yantosca (2005), Evaluating the contribution of changes in isoprene emissions to surface ozone trends over the eastern United States, *J. Geophys. Res.*, *110*, D12303, doi:10.1029/2004JD005485.

Fusco, A. C., and J. A. Logan (2003), Analysis of 1970–1995 trends in tropospheric ozone at Northern Hemisphere midlatitudes with the GEOS-CHEM model, *J. Geophys. Res.*, *108*(D15), 4449, doi:10.1029/2002JD002742.

Giacopelli, P., K. Ford, C. Espada, and P. B. Shepson (2005), Comparison of the measured and simulated isoprene nitrate distributions above a forest canopy, *J. Geophys. Res.*, *110*, D01304, doi:10.1029/2004JD005123.

Grossenbacher, J. W., et al. (2001), Measurements of isoprene nitrates above a forest canopy, *J. Geophys. Res.*, *106*(D20), 24,429–24,438.

Gupta, M. L., R. J. Cicerone, and S. Elliott (1998), Perturbation to global tropospheric oxidizing capacity due to latitudinal redistribution of surface sources of NO_x, CH_4, and CO, *Geophys. Res. Lett.*, *25*, 3931–3934.

Hack, J. J. (1994), Parameterization of moist convection in the National Center for Atmospheric Research Community Climate Model (CCM2), *J. Geophys. Res.*, *99*, 5551–5568.

Hauglustaine, D. A., G. P. Brasseur, S. Walters, P. J. Rasch, J.-F. Muller, L. K. Emmons, and M. A. Carroll (1998), MOZART, a global chemical transport model for ozone and related chemical tracers: 2. Model results and evaluation, *J. Geophys. Res.*, *103*, 28,291–28,335.

Hauglustaine, D. A., F. Hourdin, L. Jourdain, M.-A. Filiberti, S. Walters, J.-F. Lamarque, and E. A. Holland (2004), Interactive chemistry in the Laboratoire de Météorologie Dynamique general circulation model: Description and background tropospheric chemistry evaluation, *J. Geophys. Res.*, *109*, D04314, doi:10.1029/2003JD003957.

Holtslag, A. A. M., and B. Boville (1993), Local versus nonlocal boundary-layer diffusion in a global climate model, *J. Clim.*, *6*, 1825–1842.

Horowitz, L. W., J. Liang, G. M. Gardner, and D. J. Jacob (1998), Export of reactive nitrogen from North America during summertime: Sensitivity to hydrocarbon chemistry, *J. Geophys. Res.*, *103*, 13,451–13,476.

Horowitz, L. W., et al. (2003), A global simulation of tropospheric ozone and related tracers: Description and evaluation of MOZART, version 2, *J. Geophys. Res.*, *108*(D24), 4784, doi:10.1029/2002JD002853.

Houweling, S., F. Dentener, and J. Lelieveld (1998), The impact of nonmethane hydrocarbon compounds on tropospheric photochemistry, *J. Geophys. Res.*, *103*, 10,673–10,696.

Hudman, R. C., et al. (2007), Surface and lightning sources of nitrogen oxides over the United States: magnitudes, chemical evolution, and outflow, *J. Geophys. Res.*, doi:10.1029/2006JD007912, in press.

Krol, M., P. J. van Leeuwen, and J. Lelieveld (1998), Global OH trends inferred from methyl-chloroform measurements, *J. Geophys. Res.*, *103*, 10,697–10,711.

Lawrence, M. G., P. J. Crutzen, P. J. Rasch, B. E. Eaton, and N. M. Mahowald (1999), A model for studies of tropospheric photochemistry: Description, global distributions, and evaluation, *J. Geophys. Res.*, *104*, 26,245–26,278.

Lawrence, M. G., R. von Kuhlmann, M. Salzmann, and P. J. Rasch (2003), The balance of effects of deep convective mixing on tropospheric ozone, *Geophys. Res. Lett.*, *30*(18), 1940, doi:10.1029/2003GL017644.

Lelieveld, J., and F. J. Dentener (2000), What controls tropospheric ozone?, *J. Geophys. Res.*, *105*, 3531–3551.

Levy, H., II, W. J. Moxim, and P. S. Kasibhatla (1996), A global three-dimensional time-dependent lightning source of tropospheric NO_x, *J. Geophys. Res.*, *101*, 22,911–22,922.

Li, Q., et al. (2005), North American pollution outflow and the trapping of convectively lifted pollution by upper-level anticyclone, *J. Geophys. Res.*, *110*, D10301, doi:10.1029/2004JD005039.

Liang, J., et al. (1998), Seasonal variations of reactive nitrogen species and ozone over the United States, and export fluxes to the global atmosphere, *J. Geophys. Res.*, *103*, 13,435–13,450.

Lin, X., M. Trainer, and S. C. Liu (1988), On the nonlinearity of the tropospheric ozone production, *J. Geophys. Res.*, *93*(D12), 15,879–15,888.

Liu, H., et al. (2001), Constraints from ^{210}Pb and ^{7}Be on wet deposition and transport in a global three-dimensional chemical tracer model driven by assimilated meteorological fields, *J. Geophys. Res.*, *106*, 12,109–12,128.

Liu, H., et al. (2004), Constraints on the sources of tropospheric ozone from ^{210}Pb-^{7}Be-O_3 correlations, *J. Geophys. Res.*, *109*, D07306, doi:10.1029/2003JD003988.

Liu, H., et al. (2006), Radiative effect of clouds on tropospheric chemistry in a global three-dimensional chemical transport model, *J. Geophys. Res.*, *111*, D20303, doi:10.1029/2005JD006403.

Liu, X., et al. (2006), First directly retrieved global distribution of tropospheric column ozone from GOME: Comparison with the GEOS-CHEM model, *J. Geophys. Res.*, *111*, D02308, doi:10.1029/2005JD006564.

Logan, J. A. (1999), An analysis of ozonesonde data for the troposphere: Recommendations for testing 3-D models and development of a gridded climatology for tropospheric ozone, *J. Geophys. Res.*, *104*, 16,115–16,149.

Martin, R. V., et al. (2002), Interpretation of TOMS observations of tropical tropospheric ozone with a global model and in situ observations, *J. Geophys. Res.*, *107*(D18), 4351, doi:10.1029/2001JD001480.

Martin, R. V., et al. (2003a), Global inventory of nitrogen oxide emissions constrained by space-based observations of NO_2 columns, *J. Geophys. Res.*, *108*(D17), 4537, doi:10.1029/2003JD003453.

Martin, R. V., et al. (2003b), Global and regional decreases in tropospheric oxidants from photochemical effects of aerosols, *J. Geophys. Res.*, *108*(D3), 4097, doi:10.1029/2002JD002622.

McLinden, C. A., et al. (2000), Stratospheric ozone in 3-D models: A simple chemistry and the cross-tropopause flux, *J. Geophys. Res.*, *105*, 14,653–14,665.

Mickley, L. J., et al. (1999), Radiative forcing from tropospheric ozone calculated with a unified chemistry-climate model, *J. Geophys. Res.*, *104*, 30,153–30,172.

Moorthi, S., and M. J. Suarez (1992), Relaxed Arakawa-Schubert: A parameterization of moist convection for general circulation models, *Mon. Weather Rev.*, *120*, 978–1002.

Murphy, D. M., and D. W. Fahey (1994), An estimate of the flux of stratospheric reactive nitrogen and ozone into the troposphere, *J. Geophys. Res.*, *99*(D3), 5325–5332.

Olsen, S. C., C. A. McLinden, and M. J. Prather (2001), Stratospheric N_2O-NO_y system: Testing uncertainties in a three-dimensional framework, *J. Geophys. Res.*, *106*(D22), 28,771–28,784.

Park, R. J., et al. (2004a), Natural and transboundary pollution influences on sulfate-nitrate-ammonium aerosols in the United States: Implications for policy, *J. Geophys. Res.*, *109*, D15204, doi:10.1029/2003JD004473.

Park, R. J., K. E. Pickering, D. J. Allen, G. L. Stenchikov, and M. S. Fox-Rabinovitz (2004b), Global simulation of tropospheric ozone using the University of Maryland Chemical Transport Model (UMD-CTM): 1. Model description and evaluation, *J. Geophys. Res.*, *109*, D09301, doi:10.1029/2003JD004266.

Pickering, K. E., A. M. Thompson, J. R. Scala, W.-K. Tao, R. R. Dickerson, and J. Simpson (1992), Free tropospheric ozone production following entrainment of urban plumes into deep convection, *J. Geophys. Res.*, *97*, 17,985–18,000.

Pickering, K. E., Y. Wang, W. Tao, C. Price, and J. Müller (1998), Vertical distributions of lightning NOx for use in regional and global chemical transport models, *J. Geophys. Res.*, *103*(D23), 31,203–31,216.

Poisson, N., M. Kanakidou, and P. J. Crutzen (2000), Impact of nonmethane hydrocarbons on tropospheric chemistry and the oxidizing power of the global troposphere: 3-dimensional modeling results, *J. Atmos. Chem.*, *36*, 157–230.

Prather, M., et al. (2001), Atmospheric chemistry and greenhouse gases, in *Climate Change 2001: The Scientific Basis—Contribution of Working*

Group I to the Third Assessment Report of the Intergovernmental Panel on Climate Change, edited by J. T. Houghton et al., pp. 239–288, Cambridge Univ. Press, New York.

Price, C., and D. Rind (1992), A simple lightning parameterization for calculating global lightning distributions, *J. Geophys. Res.*, *97*, 9919–9933.

Price, C., J. Penner, and M. Prather (1997), NO_x from lightning: 1. Global distribution based on lightning physics, *J. Geophys. Res.*, *102*, 5929–5941.

Prinn, R. G., et al. (2005), Evidence for variability of atmospheric hydroxyl radicals over the past quarter century, *Geophys. Res. Lett.*, *32*, L07809, doi:10.1029/2004GL022228.

Rind, D., J. Lerner, K. Shah, and R. Suozzo (1999), Use of on-line tracers as a diagnostic tool in general circulation model development: 2. Transport between the troposphere and stratosphere, *J. Geophys. Res.*, *104*, 9151–9167.

Roelofs, G.-J., and J. Lelieveld (1997), Model study of the influence of cross-tropopause O_3 transports on tropospheric O_3 levels, *Tellus, Ser. B*, *49*, 38–55.

Roelofs, G.-J., and J. Lelieveld (2000), Tropospheric ozone simulation with a chemistry-general circulation model: Influence of higher hydrocarbon chemistry, *J. Geophys. Res.*, *105*, 22,697–22,712.

Rotman, D. A., et al. (2004), IMPACT, the LLNL 3-D global atmospheric chemical transport model for the combined troposphere and stratosphere: Model description and analysis of ozone and other trace gases, *J. Geophys. Res.*, *109*, D04303, doi:10.1029/2002JD003155.

Shindell, D. T., G. Faluvegi, and N. Bell (2003), Preindustrial-to-present-day radiative forcing by tropospheric ozone from improved simulations with the GISS chemistry-climate GCM, *Atmos. Chem. Phys.*, *3*, 1675–1702.

Sillman, S., J. A. Logan, and S. C. Wofsy (1990), The sensitivity of ozone to nitrogen oxides and hydrocarbons in regional ozone episodes, *J. Geophys. Res.*, *95*(D2), 1837–1851.

Spivakovsky, C. M., et al. (2000), Three-dimensional climatological distribution of tropospheric OH: Update and evaluation, *J. Geophys. Res.*, *105*, 8931–8980.

Sprengnether, M., K. L. Demerjian, N. M. Donahue, and J. G. Anderson (2002), Product analysis of the OH oxidation of isoprene and 1,3-butadiene in the presence of NO, *J. Geophys. Res.*, *107*(D15), 4268, doi:10.1029/2001JD000716.

Stevenson, D. S., et al. (1997), The impact of aircraft nitrogen oxide emissions on tropospheric ozone studied with a 3D Lagrangian model including fully diurnal chemistry, *Atmos. Environ.*, *31*, 1837–1850.

Stevenson, D. S., et al. (2000), Future tropospheric ozone radiative forcing and methane turnover: The impact of climate change, *Geophys. Res. Lett.*, *27*, 2073–2076.

Stevenson, D. S., et al. (2004), Radiative forcing from aircraft NO_x emissions: Mechanisms and seasonal dependence, *J. Geophys. Res.*, *109*, D17307, doi:10.1029/2004JD004759.

Stevenson, D. S., et al. (2006), Multimodel ensemble simulations of present-day and near-future tropospheric ozone, *J. Geophys. Res.*, *111*, D08301, doi:10.1029/2005JD006338.

Sudo, K., M. Takahashi, and H. Akimoto (2002), CHASER: A global chemical model of the troposphere: 2. Model results and evaluation, *J. Geophys. Res.*, *107*(D21), 4586, doi:10.1029/2001JD001114.

Tan, W. W., M. A. Geller, S. Pawson, and A. da Silva (2004), A case study of excessive subtropical transport in the stratosphere of a data assimilation system, *J. Geophys. Res.*, *109*, D11102, doi:10.1029/2003JD004057.

Tie, X. X., R. Y. Zhang, G. Brasseur, and W. F. Lei (2002), Global NO_x production by lightning, *J. Atmos. Chem.*, *43*(1), 61–74.

Tie, X., S. Madronich, S. Walters, D. P. Edwards, P. Ginoux, N. Mahowald, R. Zhang, C. Lou, and G. Brasseur (2005), Assessment of the global impact of aerosols on tropospheric oxidants, *J. Geophys. Res.*, *110*, D03204, doi:10.1029/2004JD005359.

van Noije, T. P. C., H. J. Eskes, M. van Weele, and P. F. J. van Velthoven (2004), Implications of the enhanced Brewer-Dobson circulation in European Centre for Medium-Range Weather Forecasts reanalysis ERA-40 for the stratosphere-troposphere exchange of ozone in global chemistry transport models, *J. Geophys. Res.*, *109*, D19308, doi:10.1029/2004JD004586.

von Kuhlmann, R., M. G. Lawrence, P. J. Crutzen, and P. J. Rasch (2003), A model for studies of tropospheric ozone and nonmethane hydrocarbons: Model description and ozone results, *J. Geophys. Res.*, *108*(D9), 4294, doi:10.1029/2002JD002893.

von Kuhlmann, R., M. G. Lawrence, U. Pöschl, and P. J. Crutzen (2004), Sensitivities in global scale modeling of isoprene, *Atmos. Chem. Phys.*, *4*, 1–17.

Wang, Y., and D. J. Jacob (1998), Anthropogenic forcing on tropospheric ozone and OH since preindustrial times, *J. Geophys. Res.*, *103*, 31,123–31,135.

Wang, Y., D. J. Jacob, and J. A. Logan (1998a), Global simulation of tropospheric O_3-NOx-hydrocarbon chemistry: 1. Model formulation, *J. Geophys. Res.*, *103*, 10,713–10,725.

Wang, Y., J. A. Logan, and D. J. Jacob (1998b), Global simulation of tropospheric O_3-NOx-hydrocarbon chemistry: 2. Model evaluation and global ozone budget, *J. Geophys. Res.*, *103*, 10,727–10,755.

Wang, Y., D. J. Jacob, and J. A. Logan (1998c), Global simulation of tropospheric O_3-NO_x-hydrocarbon chemistry: 3. Origin of tropospheric ozone and effects of nonmethane hydrocarbons, *J. Geophys. Res.*, *103*, 10,757–10,767.

Wauben, W. M., et al. (1998), Comparison of modeled ozone distributions with sonde and satellite observations, *J. Geophys. Res.*, *103*, 3511–3530.

Wild, O., and M. J. Prather (2000), Excitation of the primary tropospheric chemical mode in a global CTM, *J. Geophys. Res.*, *105*, 24,647–24,660.

Wild, O., X. Zhu, and M. J. Prather (2000), Fast-J: Accurate simulation of in- and below-cloud photolysis in tropospheric chemical models, *J. Atmos. Chem.*, *37*, 245–282.

Wild, O., P. Pochanart, and H. Akimoto (2004), Trans-Eurasian transport of ozone and its precursors, *J. Geophys. Res.*, *109*, D11302, doi:10.1029/2003JD004501.

Wong, S., et al. (2004), A global climate-chemistry model study of present-day tropospheric chemistry and radiative forcing from changes in tropospheric O_3 since the preindustrial period, *J. Geophys. Res.*, *109*, D11309, doi:10.1029/2003JD003998.

Zender, C. S., H. Bian, and D. Newman (2003), Mineral Dust Entrainment and Deposition (DEAD) model: Description and 1990s dust climatology, *J. Geophys. Res.*, *108*(D14), 4416, doi:10.1029/2002JD002775.

Zhang, G. J., and N. A. McFarlane (1995), Sensitivity of climate simulations to the parameterization of cumulus convection in the Canadian Climate Centre general circulation model, *Atmos. Ocean*, *33*(3), 407–446.

D. J. Jacob, J. A. Logan, L. J. Mickley, S. Wu, and R. M. Yantosca, Division of Engineering and Applied Sciences and Department of Earth and Planetary Sciences, Harvard University, Cambridge, MA 02138, USA. (wu18@fas.harvard.edu)

D. Rind, NASA Goddard Institute for Space Studies, New York, NY 10025, USA.